J Neurophysiol 112: 446–462, 2014.
First published April 16, 2014; doi:10.1152/jn.00796.2013.

A potentially novel nicotinic receptor in *Aplysia* neuroendocrine cells

Sean H. White, Christopher J. Carter, and Neil S. Magoski
Department of Biomedical and Molecular Sciences, Physiology Graduate Program, Centre for Neuroscience Studies, Queen's University, Kingston, Ontario, Canada

Submitted 7 November 2013; accepted in final form 15 April 2014

White SH, Carter CJ, Magoski NS. A potentially novel nicotinic receptor in *Aplysia* neuroendocrine cells. *J Neurophysiol* 112: 446–462, 2014. First published April 16, 2014; doi:10.1152/jn.00796.2013.—Nicotinic receptors form a diverse group of ligand-gated ionotropic receptors with roles in both synaptic transmission and the control of excitability. In the bag cell neurons of *Aplysia*, acetylcholine activates an ionotropic receptor, which passes inward current to produce a long-lasting afterdischarge and hormone release, leading to reproduction. While testing the agonist profile of the cholinergic response, we observed a second current that appeared to be gated only by nicotine and not acetylcholine. The peak nicotine-evoked current was markedly smaller in magnitude than the acetylcholine-induced current, cooperative (Hill value of 2.7), had an EC_{50} near 500 μM, readily recovered from desensitization, showed Ca^{2+} permeability, and was blocked by mecamylamine, dihydro-β-erythroidine, or strychnine, but not by α-conotoxin ImI, methyllycaconitine, or hexamethonium. *Aplysia* transcriptome analysis followed by PCR yielded 20 full-length potential nicotinic receptor subunits. Sixteen of these were predicted to be cation selective, and real-time PCR suggested that 15 of the 16 subunits were expressed to varying degrees in the bag cell neurons. The acetylcholine-induced current, but not the nicotine current, was reduced by double-strand RNA treatment targeted to both subunits ApAChR-C and -E. Conversely, the nicotine-evoked current, but not the acetylcholine current, was lessened by targeting both subunits ApAChR-H and -P. To the best of our knowledge, this is the first report suggesting that a nicotinic receptor is not gated by acetylcholine. Separate receptors may serve as a means to differentially trigger plasticity or safeguard propagation by assuring that only acetylcholine, the endogenous agonist, initiates large enough responses to trigger reproduction.

acetylcholine receptor; α-conotoxin ImI; Ca^{2+} permeability; desensitization; mollusc

THE PENTAMERIC LIGAND-GATED ion channel superfamily is a large group of receptors with a common structure. Vertebrate receptors of this type possess an extracellular disulfide-bonded cys-loop and are gated by acetylcholine, glycine, λ-aminobutyric acid (GABA), serotonin, or zinc (Albuquerque et al. 2009; Thompson et al. 2010). Invertebrate receptors also have a cys-loop and bind not only acetylcholine and GABA, but also glutamate and histamine (Jones and Sattelle 2007; Kehoe et al. 2009; Norekian 1999). Some prokaryotic versions are gated by H^+ and GABA but lack the cys-loop (Corringer et al. 2010). The best studied of these channels are the nicotinic receptors, which, despite acetylcholine being the endogenous ligand, are categorized by nicotine binding. That stated, there are examples of cholinergic ionotropic receptors being both nicotine insensitive and acetylcholine sensitive, such as in the nematode *Caenorhabditis elegans* (Richmond and Jorgensen 1999) and the mollusc *Aplysia californica* (Kehoe and McIntosh 1998), as well as chicken $\alpha3\beta2$ (Hussy et al. 1994) and mammalian $\alpha9$ receptors (Elgoyhen et al. 1994; Rothlin et al. 1999) in expression systems. However, there are no prior reports of nicotinic ionotropic receptors failing to respond to acetylcholine. In the present study, we provide evidence for ionotropic receptors in *Aplysia* neuroendocrine cells: one activated by nicotine alone and the other by acetylcholine alone.

The bag cell neurons are neuroendocrine cells that control reproduction in the marine snail, *A. californica*. They are found in two clusters just rostral to the abdominal ganglion and in response to acetylcholine undergo an ~30-min afterdischarge of depolarization and spiking (Ferguson et al. 1989; Kauer and Kaczmarek 1985; Kupfermann and Kandel 1970; White and Magoski 2012). During the afterdischarge, hormones are released into the blood to initiate egg-laying behavior (Arch 1972; Chiu et al. 1979; Sigvardt et al. 1986). Aside from an example of a metabotropically gated K^+ channel (Kehoe 1994), the vast majority of responses to acetylcholine in *Aplysia* neurons are ionotropic and inhibitory. However, in some neurons, such as the small unpigmented cells of the pleural ganglion, the RB cluster of the abdominal ganglion, and the bag cell neurons themselves, acetylcholine generates depolarization (Bodmer and Levitan 1984; Kehoe and McIntosh 1998; Simmons and Koester 1986; White and Magoski 2012).

While characterizing the bag cell neuron cholinergic ionotropic receptor, we found that nicotine failed to reproduce the acetylcholine response (White and Magoski 2012). Rather, nicotine induced a second cationic response not mimicked by acetylcholine. In this article we propose that these two currents are mediated by disparate receptors, on the basis of magnitude, desensitization, antagonist profile, Ca^{2+} permeability, and RNA inhibition. This may represent a unique example of two cholinergic ionotropic receptors on the same neuron responding to different ligands. Such receptor diversity might allow for discrete activation of signaling pathways or be an adaptation that ensures reproductive success in the face of marine venoms and toxins that act as nicotinic agonists and antagonists (Bourne et al. 2010; Dwoskin and Crooks 2001; Kem 1997; Schwarz et al. 2003).

MATERIALS AND METHODS

Animals and cell culture. Adult *A. californica* (a hermaphrodite) weighing 150–500 g were obtained from Marinus (Long Beach, CA), housed in an ~300-liter aquarium containing continuously circulating, aerated artificial sea water (Instant Ocean; Aquarium Systems, Mentor, OH) at 15°C on a 12:12-h light-dark cycle, and fed Romaine lettuce 5 times a week. For primary cultures of isolated bag cell neurons, animals were anesthetized by an injection of isotonic $MgCl_2$ (~50% body wt), and the abdominal ganglion was removed and

Address for reprint requests and other correspondence: N. S. Magoski, Dept. of Biomedical and Molecular Sciences, Queen's Univ., 4th Floor, Botterell Hall, 18 Stuart St., Kingston, ON, Canada K7L 3N6 (e-mail: magoski@queensu.ca).

treated with neutral protease (13.33 mg/ml; catalog no. 165859; Roche Diagnostics, Indianapolis, IN) dissolved in tissue culture artificial sea water (tcASW; composition in mM: 460 NaCl, 10.4 KCl, 11 $CaCl_2$, 55 $MgCl_2$, 15 HEPES, 1 mg/ml glucose, 100 U/ml penicillin, and 0.1 mg/ml streptomycin; pH 7.8 with NaOH) for 18 h at 20–22°C. The ganglion was then rinsed in tcASW for 1 h, after which the bag cell neuron clusters were dissected from their connective tissue. With the use of a fire-polished Pasteur pipette and gentle trituration, neurons were dispersed in tcASW onto 35 × 10-mm polystyrene tissue culture dishes (catalog no. 353001; Falcon Becton-Dickinson, Franklin Lakes, NJ). Cultures were maintained in a 14°C incubator and used within 1–3 days. Salts were obtained from Fisher Scientific (Ottawa, ON, Canada), ICN (Aurora, OH), or Sigma-Aldrich (St. Louis, MO).

Sharp-electrode current-clamp and whole cell voltage-clamp recording. Current-clamp recordings were made from cultured bag cell neurons in normal artificial seawater (nASW; composition as per tcASW but lacking the glucose and antibiotics) using an AxoClamp 2B amplifier (Axon Instruments/Molecular Devices, Sunnyside, CA) and the sharp-electrode, bridge-balanced method. Microelectrodes were pulled from 1.2-mm external, 0.9-mm internal diameter borosilicate glass capillaries (item no. TW120F-4; World Precision Instruments, Sarasota, FL) and had a resistance of 5–20 MΩ when filled with 2 M K-acetate plus 10 mM HEPES and 100 mM KCl (pH 7.3 with KOH). Current was delivered with either Clampex software (version 8 or 10; Molecular Devices) or a Grass S88 stimulator (Astro-Med, Longueuil, QC, Canada). Voltage was filtered at 3 kHz using the AxoClamp Bessel filter and sampled at 2 kHz using a Digidata 1322A analog-to-digital converter (Molecular Devices), Clampex, and an IBM-compatible personal computer.

Voltage-clamp recordings were made from cultured bag cell neurons using an EPC-8 amplifier (HEKA Electronics, Mahone Bay, NS, Canada) and the tight-seal, whole cell method. Microelectrodes were pulled from 1.5-mm external, 1.2-mm internal diameter borosilicate glass capillaries (item no. TW150F-4; World Precision Instruments) and had a resistance of 1–2 MΩ when fire-polished and filled with regular intracellular saline (see below). Before seal formation, pipette junction potentials were nulled. After seal formation, the pipette capacitive current was canceled, and following breakthrough, the whole cell capacitive current was also canceled, while the series resistance (3–5 MΩ) was compensated to 80% and monitored throughout the experiment. Current was filtered at 1 kHz with the EPC-8 Bessel filter and sampled at 2 kHz as per current clamp. Data were gathered at room temperature (20–22°C).

Most voltage-clamp recordings were made in nASW, although in some cases Ca^{2+} was replaced with Mg^{2+} and 0.5 mM EGTA added to achieve Ca^{2+}-free ASW. The recording pipette was filled with standard intracellular saline [composition in mM: 500 K-aspartate, 70 KCl, 1.25 $MgCl_2$, 10 HEPES, 11 glucose, 10 glutathione, 5 EGTA, ATP disodium salt hydrate (A3377; Sigma-Aldrich), and 0.1 GTP sodium salt hydrate (catalog no. G8877; Sigma-Aldrich); pH 7.3 with KOH]. In some instances, the K^+ was replaced with Cs^+ or the GTP was replaced with 10 mM guanosine 5′-[β-thio]diphosphate trilithium salt (GDPβS; catalog no. G7637; Sigma-Aldrich). The free intracellular Ca^{2+} concentration was set at 300 nM by adding the appropriate amount of $CaCl_2$, as calculated using WebMaxC (http://www.stanford.edu/~cpatton/webmaxcS.htm). A junction potential of 15 mV was calculated for intracellular saline vs. nASW and compensated for by subtraction off-line.

Ca^{2+} imaging. Ca^{2+} imaging was performed under whole cell voltage-clamp using the standard intracellular saline, but supplemented with 1 mM of the Ca^{2+}-sensitive dye fura PE3 (Vorndran et al. 1995) and with the EGTA and Ca^{2+} removed. After breakthrough, neurons were dye-filled by being dialyzed for at least 10 min. Imaging was performed using a Nikon TS100-F inverted microscope (Nikon, Mississauga, ON, Canada) equipped with a Nikon Plan Fluor ×20 (numerical aperture 0.5) objective. The light source was a 75-W Xenon arc lamp and a multiwavelength DeltaRAM V monochromatic illuminator (Photon Technology International, London, ON, Canada) coupled to the microscope with a UV-grade liquid-light guide. Excitation wavelengths were 340 and 380 nm. Between acquisition episodes, the excitation illumination was blocked by a shutter, which along with the excitation wavelength was controlled by an IBM-compatible computer, a Photon Technology International computer interface, and EasyRatioPro software (version 1.10; Photon Technology International). The emitted light passed through a 400-nm dichroic mirror and a 510/40-nm emission barrier filter before being detected by a CoolSNAP HQ^2 ICX285 charge-coupled device camera (Photometrics, Tucson, AZ). The high threshold value was left at maximum and, to reduce background, the low threshold value was set to 400 arbitrary units of fluorescence. From a focal plane near the middle of the neuron, fluorescence intensities were sampled using a region of interest defined over the soma at 2-s intervals and averaged 8 frames/acquisition. The ratio of the emission following 340- and 380-nm excitation (340/380) was taken to reflect free intracellular Ca^{2+} and saved for subsequent analysis. Threshold level, image acquisition, frame averaging, region of interest sampling, and ratio calculations were carried out using EasyRatioPro.

Drug application and reagents. The culture dish served as the bath, with transmitters and drugs applied using either single-cell microperfusion or pressure ejection. The perfusion system consisted of a micromanipulator-controlled square-barreled glass pipette (~500-μm bore) positioned 300–500 μm from the soma and connected by a stopcock manifold to a series of gravity-driven reservoirs. This provided a constant flow (~0.5–1 ml/min) of control extracellular saline over the neuron, which was switched to agonist-containing saline by activating the appropriate stopcock. Additional experiments involved pressure ejection of an agonist from an unpolished patch pipette (1- to 2-μm bore, positioned ~10 μm from the soma) for 2 s at 75–150 kPa using a PMI-100 pressure microinjector (Dagan, Minneapolis, MN). For antagonists, the blocker was introduced directly into the bath by pipetting a small volume of concentrated stock solution before pressure application. As previously undertaken with bag cell neurons by Fisher et al. (1993) and our laboratory (White and Magoski 2012), perfusion was, with one exception, not employed during pressure application; however, the pipette was removed from the bath immediately after each ejection to minimize leakage and possible desensitization.

Stock solutions of drugs were made in water, frozen at −20°C, and then diluted to a working concentration in the appropriate extracellular saline as needed: acetylcholine chloride (catalog no. A6625; Sigma-Aldrich), α-conotoxin ImI (catalog no. 3119; Tocris Bioscience), dihydro-β-erythroidine hydrobromide (catalog no. D149; Sigma-Aldrich), 1,1-dimethyl-4-phenylpiperazinium iodide (DMPP; catalog no. D5891; Sigma-Aldrich), hexamethonium bromide (catalog no. H2138; Sigma-Aldrich), mecamylamine hydrochloride (catalog no. M9020; Sigma-Aldrich), methyllycaconitine citrate salt hydrate (MLA; catalog no. M168; Sigma-Aldrich), nicotine (catalog no. N0257; Sigma-Aldrich), strychnine (catalog no. S0532; Sigma-Aldrich), and tetramethylammonium chloride (TMA; catalog no. T19526; Sigma-Aldrich).

In silico identification of cholinergic ionotropic receptor subunits. We initially searched for putative *Aplysia* receptor subunits in the University of California Santa Cruz Sea Hare Genome Browser (http://genome.ucsc.edu/, September 2008 Broad 2.0/aplCal1 assembly) by employing the BLAST-like alignment tool (BLAT) with published acetylcholine receptor (AChR) subunit sequences from another mollusc, *Lymnaea stagnalis* (van Nierop et al. 2006). The BLAT queries used the following published *Lymnaea* receptor subunits: LnAChR-A (GenBank accession no. DQ167344), LnAChR-B (DQ167345), LnAChR-C (DQ167346), LnAChR-D (DQ167347), LnAChR-E (DQ167348), LnAChR-F (DQ16734), LnAChR-G (DQ167350), LnAChR-H (DQ167351), LnAChR-I (DQ167352), LnAChR-J (DQ167354), LnAChR-K (DQ167353) and LnAChR-L

nic = N0267

(DQ167355). This yielded 12 predicted partial sequences of equivalent *Aplysia* receptors (ApAChR-A to -L). We lengthened these ApAChR sequences with Prot2Gene (courtesy of Dr. P. Liang, Brock University, St. Catharines, ON, Canada; http://genomics.brocku.ca/Prot2gene/), which allowed for precise exon prediction and mapping with large stretches of the *Aplysia* genome and full or nearly full LnAChR protein sequences as input. Using the deep RNA sequencing project and large transcriptome shotgun assembly of the *Lymnaea* central nervous system (CNS) (Sadamoto et al. 2012), we also found previously unidentified putative LnAChR subunits, namely, LnAChR-J2 (DNA Database of Japan accession no. FX184869), LnAChR-J3 (FX182518), LnAChR-K2 (FX183719), LnAChR-M (FX180550), LnAChR-O (FX183843), LnAChR-P (FX222775-partial), LnAChR-Q (FX182529), and LnAChR-R (FX183247) (contigs from the *Lymnaea* transcriptome shotgun assembly are available at http://www.ddbj.nig.ac.jp). Homologs of these additional AChRs were then found in *Aplysia* by BLAST search of an *Aplysia* RNA sequence assembly from the Institute for Genome Sciences at the University of Maryland (http://aplysiagenetools.org). In total, we identified 15 new putative *Aplysia* full-length cation-selective subunits (ApAChR A, C, D, E, G, H, J2, J3, L, M, N, O, P, Q, and R) and 5 anionic-selective subunits (ApAChR B, F, I, K1, and K2). A sixteenth putative cation-selective subunit, which we have designated ApAChR-J1, was previously published in GenBank as accession number NP_001191486 (Moroz et al. 2006).

PCR of full-length sequences. Abdominal ganglia were dissected from *Aplysia* and the bag cell neuron clusters removed. Ganglia were snap-frozen in liquid N_2 and homogenized in lysis solution from a Norgen Total RNA isolation kit (catalog no. 17200; Norgen Biotek, Thorold, ON, Canada). Total RNA was then isolated and purified from these ganglia using the Norgen kit. cDNA was synthesized by reverse transcription with an iScript cDNA synthesis kit (catalog no. 170-8890; Bio-Rad Laboratories, Mississauga, ON, Canada) using a mixture of polyA and random hexamer primers. PCR amplification of ApAChR subunits was performed with a Techne Touchgene Gradient Thermocycler (Fisher Scientific) using 1 μl of cDNA as template, 40 pmol of forward and reverse primer sets against the 16 different cation-selective ApAChRs (Table 1), iTaq DNA polymerase (catalog

Table 1. *PCR primers for individual of Aplysia nicotinic receptor subunits*

ApAChR	Forward	Reverse
A	5′-CGAGTGATTTCCAAGGGATGCTGAG-3′	5′-CTCTGGGCAGCAGTCGTACTGGAGA-3′
	5′-CTTACGTAGGGGGCCTGCTGAACCT-3′	5′-CCCTCTGTGTCAGTGACCTCCGTGT-3′
	5′-TGAACTTTCACTACCGCTCGCCTGA-3′	5′-AGCCACACCTTCCTCGCTAGCCTCT-3′
C	5′-ACGAGGGGGAAACAAGCTTGGAAAC-3′	5′-CAGCTCGTCTCCGTGGTATGTCCAG-3′
	5′-ACAACGCCGACGGAGACTTTCAGAT-3′	5′-AAAACACAGTGAGGGCGAGCAGGAT-3′
	5′-TGCGACGACGCACACTGTTCTACAC-3′	5′-CCCCAAAAGGAAGGCCATGGCATAAT-3′
D	5′-CCATAGGTGCCATGGTACACCAGCAT-3′	5′-TCCGAGAGTGACTTTCTCTCCTGAGTC-3′
	5′-CTCACTCACGCTCCTCGTGTTTTGG-3′	5′-CACTGGGAAGTTGTGACTTGTTGACG-3′
E	5′-TCACACAAGGCTTGGTGGCTCCGTC-3′	5′-GTGATCTTCTCGCCCGAGTCTGAGG-3′
	5′-CATGTGTGGCCATCTCCTTCCTCAC-3′	5′-ATACTAGACATGAGATATTCGATCT-3′
G	5′-GACATGCAGCAATGCACCCATTTG-3′	5′-GCCTGCGGATTCGGACATCTATGAG-3′
	5′-ATCTTGCGCATCCCTTGTGAGAAGC-3′	5′-GTCATGCCCATTGTCACCGTCAGAT-3′
	5′-GGCATGACCTCAATGTCCATCATCC-3′	5′-AAAGGTGTGTGTCCCCCAAAGTGTG-3′
H	5′-GACACCAGCCCGCTATACCGTCAAC-3′	5′-GTGAGGGTAGGGGTCTGGACAGCAG-3′
	5′-CTGCTGTCCAGACCCCTACCCTCAC-3′	5′-GTCCGGGAACTCGACAAGCTGTCTT-3′
J2	5′-CAGCAGACATCACTGAGGGTTTTGAC-3′	5′-CCGTCATGGCGTCGTCTATAGTGGT-3′
	5′-CATCCCGGCTGCTATCTACACGTCA-3′	5′-TGGGCATGACGTCAGTACGAGGAGT-3′
	5′-ATCACACTGGTCATCTCAGTGCTCGTC-3′	5′-CTCACGACTCAGGACTCAATCTTCCA-3′
J3	5′-TGGTTTACCCCTTGGTCTCGTCTTTG-3′	5′-CAAGGCTAGGAGGACGGAGATGCAG-3′
	5′-TCCTTTGTGAGCGTGTGTGTGTTCG-3′	5′-TGCGCCTTCTTGTCTCAGGTAACCA-3′
L	5′-TAGACAGTCGGGGCTCCATCTTTGC-3′	5′-GAACAAGGGCCGCCGCTTTATAAGT-3′
	5′-CGTCCACCTCGTCCAACCTTATCGT-3′	5′-ATGACCATTGGCACGGCTTTACCTC-3′
	5′-GGGGAGAAGGTGACCATGGGTATCA-3′	5′-CCAGCAGTACAACGCCTGTGATGGT-3′
M	5′-CACAAACGCCTTGGCTGTATTGGAG-3′	5′-GAGGTCAAGGACATCACGATGGTCAG-3′
	5′-CCTATTTCCCGTTCGACAGCCAAGA-3′	5′-CCAAACGAAGCTCATCCCTCAGGTC-3′
	5′-CCTGACCATCGTGATGTCCTTGACC-3′	5′-TCACGAGTCTTGTGTAGCGGGCATA-3′
N	5′-CAACTGTTGAGCCGGTTGAGGGAAT-3′	5′-GAAACACGGCAAGGGAGAGCAGAAC-3′
	5′-ACAAATGCTGTCCAGAGCCGTACCC-3′	5′-GGCCAGCTGCTGTTTGAGAACTTCC-3′
	5′-TGCCGTGTTTCTTTTGGTGGTCTCC-3′	5′-TGCCTGTTTGGGATGGAGAAAGAG-3′
O	5′-CGCTGGCTTAAGTGACTGCCTTTCA-3′	5′-CCGCAGCCATTATTAGCGACACACA-3′
	5′-GTTCCTGACACAAACACCACACCA-3′	5′-CTTGTCCCCGTTAAGTCTGCCAAAAC-3′
P	5′-GGAGTCCAAGTGCTTGTGCTGTGCT-3′	5′-CTGACTCCTCGCAGGCACCAAAAAC-3′
	5′-AGCAGCCTTTCACCCTCATCACCAT-3′	5′-CCGCTGATGCCTCCATCGAGATAAT-3′
Q	5′-CGTGGGTGTGACGTTGTACAGTTTTCC-3′	5′-AAGAGTGAGCACAGACAGCATGACG-3′
	5′-GGTGATTTACCTGAAGCGGAACACG-3′	5′-TGTTGGGACAGTTAGTACGCCTCCA-3′
	5′-TCCAAGTCACCCAACACTCGGAAGA-3′	5′-CTTTGGCTTAGCTGCTCCGCATGTA-3′
R	5′-GAGCAGCAGAAAAAGAGTGCGATG-3′	5′-GCCAGAACACCGTTCCGTCATGG-3′
	5′-CGAACGTCTGGTTGGATCAGGAATG-3′	5′-GATGGTGGCAGTTGAGCACGAAGAC-3′
	5′-AGGTCACCCTAGGCCTCACAGTGCT-3′	5′-GAGGCTTTCATTCCTCCGGGAACTC-3′

For each nicotinic acetylcholine *Aplysia* receptor (ApAChR), the first primer pair amplifies from the 5′-untranslated region through to the internal coding region of the gene, and the last primer pair amplifies from the internal coding region through to the 3′-untranslated region. For those ApAChRs where a middle primer pair is listed, it amplifies a strictly internal coding region. In all cases, the resulting PCR products overlap to provide full-length open reading frames.

no. 170-8870; Bio-Rad Laboratories), and the following program: 3 min of denaturation at 95°C, 38 cycles at 95°C for 30 s, annealing at 68°C for 30 s, and elongation at 72°C for 90 s. Analysis of products was carried out on 1% agarose gels in TAE buffer (Tris-acetate-EDTA) stained with ethidium bromide. Fragments of interest were excised from the gel, purified with an UltraClean GelSpin DNA extraction kit (catalog no. 12400; MO BIO Laboratories, Carlsbad, CA), and sequenced by GénomeQuébec (Montréal, QC, Canada) using an Applied Biosystems 3730xl DNA Analyzer. GenBank database accession numbers for the sequences are as follows: ApAChR-A (KC417388), ApAChR-C (KC411667), ApAChR-D (KC411668), ApAChR-E (KC411669), ApAChR-G (KC411660), ApAChR-H (KC411661), ApAChR-J2 (KC417389), ApAChR-J3 (KC417390), ApAChR-L (KC618637), ApAChR-M (KC618636), ApAChR-N (KC411662), ApAChR-O (KC411663), ApAChR-P (KC411664), ApAChR-Q (KC411665), and ApAChR-R (KC411666).

Real-time PCR. RNA was isolated from either *Aplysia* bag cell neuron clusters or abdominal ganglia (sans the bag cell neurons) using the Norgen Total RNA isolation kit. RNA purity was analyzed by spectrophotometry (NanoVue; GE Healthcare Bio-Sciences, Baie d'Urfe, QC, Canada), and cDNA was synthesized by reverse transcription using the iScript cDNA synthesis kit and 500 ng of total RNA with a mixture of polyA and random hexamer primers. Each forward and reverse primer (Table 2) was designed by Primer3 (http://frodo.wi.mit.edu) to generate 100- to 150-bp amplicons. Prior testing ensured that each primer pair had a 95–99% amplification efficiency with the use of a 10-fold dilution series. The 20-μl final reaction mixture contained 1 μl of cDNA, 10 μl of iQ SYBR Green Supermix (catalog no. 170-8880; Bio-Rad Laboratories), and 0.4 μmol of each primer. For both bag cell neuron and abdominal ganglion cDNA, the relative expression of each cation-selective ApAChR was estimated in triplicate. Similarly to van Nierop et al. (2005, 2006) and *Lymnaea* receptors, ApAChR expression was calculated relative to *Aplysia* glyceraldehyde 3-phosphate dehydrogenase (GAPDH) (GenBank accession no. KC417387) expression. However, the relative expression of multiple genes could be influenced by differences in primer pair efficiency and thus must be considered an estimate. Real-time PCR was performed in low-profile 96-well clear PCR multiplates (MLL-9601; Bio-Rad Laboratories) sealed with Microseal "B" film (MSB-1001; Bio-Rad Laboratories) using a Bio-Rad Laboratories CFX96 real-time PCR detection system with the following conditions: 95.0°C for 3 min, followed by 40 cycles at 95.0°C for 15 s and annealing/extension at 60.0°C for 40 s. Subsequently, PCR products were heated to 95.0°C for 15 s, and a melt curve was generated by measuring fluorescence during a temperature increase from 65.0 to 95.0°C in 0.5°C/10-s increments. Bio-Rad CFX Manager software (version 3.0) was used to generate the cycle threshold (Ct) values of the transcripts.

Double-stranded RNA treatment. To examine the impact of reducing the expression of individual ApAChR subunits on acetylcholine- or nicotine-induced currents, bag cell neurons were incubated in long double-stranded ribonucleic acid (dsRNA) (Bhargava et al. 2004; Fire et al. 1998). cDNA fragments encoding ApAChR-C (543 bp), ApAChR-E (496 bp), ApAChR-H (507 bp), and ApAChR-P (526 bp) were separately PCR amplified using iTaq DNA polymerase and gene-specific primers (AChR-C: forward, 5′-ACAACGCCGACGGAGACTTTCAGAT-3′; reverse, 5′-AAAACACAGTGAGGGCGAGCAGGAT-3′; AChR-E: 5′-TGGAGACCAAGTGGATCTGGTGCAT-3′; reverse, 5′-ACTGTGTGTGGCAGGTGATCGGAAA-3′; AChR-H: forward, 5′-CACCGCCTGTGACAACTCCGACTAC-3′; reverse, 5′-TAGTAGCTGTCGCTCCCAAGGCACA-3′; AChR-P: forward, 5′-AGCAGCCTTTCACCCTCATCACCAT-3′; reverse, 5′-TCCACTTCCTGTAAGGTCGGCTCGT-3′) extended on their 5′-ends with a T7 RNA promoter sequence (TAATACGACTCACTATAGGGAGA). With the use of 500 ng of bag cell neuron cluster cDNA (obtained as per *PCR of full-length sequences*), 5 cycles of PCR were performed with melting at 95°C for 30 s, annealing at 68°C for 30 s, and elongation at 72°C for 50 s, followed by 30 cycles of PCR with melting at 95°C for 30 s, annealing at 72°C for 30 s, and elongation at 72°C for 50 s. The PCR product was agarose gel purified with an UltraClean GelSpin DNA extraction kit and used to synthesize sense and antisense cRNA in the same reaction mix with T7 RNA polymerase (4 h at 37°C) from a MEGAscript RNAi kit (AM1626; Life Technologies, Burlington, ON, Canada). Reactions were treated with DNaseI and RNase (both from the MEGAscript kit) for 1 h at 37°C and column purified according to the MEGAscript kit protocol. As a negative control, a 450-bp dsRNA was prepared directed against the 5′-untranslated region of the newt (*Notophthalmus viridescens*) retinoic acid receptor (GenBank accession no. AY847515) using gene-specific primers (forward, 5′-AGCATGGACCGATCCTAGAG-3′; reverse, 5′-GTTGGGTTCCGTACTGAGGA-3′) with T7 ends. Bag cell neurons were first cultured overnight at 14°C and then bath-incubated at 14°C in 600 ng/ml dsRNA for an additional 3–4 days. This method of long dsRNA treatment has been successfully employed to knock down gene and protein expression in *Aplysia* bag cell (Hickey et al. 2013) and sensory neurons (Lee et al. 2009), as well as *Lymnaea* motor neurons (van Kesteren et al. 2006).

Amino acid sequence analysis and phylogenetic tree generation. Amino acid sequences were translated from nucleotide sequences and aligned using multiple sequence comparison by log-expectation (MUSCLE) (Edgar 2004) with the default settings in Jalview 2.8 (Waterhouse et al. 2009). Proposed signal peptide sequences were identified with SignalP 4.1

Table 2. *Real-time PCR primers for individual of Aplysia nicotinic receptor subunits and GAPDH*

	Forward	Reverse
A	5′-ATGACTTGGCATGCCTACAAC-3′	5′-GGCGCTGTTGTACATGAGAAT-3′
C	5′-GAAAACCAAAGCGATCGTGTA-3′	5′-AGGAGCTGATCTTGAGGAAGC-3′
D	5′-TGACGTGATCTTCACAATCCA-3′	5′-GACTCATCCAAAACACGAGGA-3′
E	5′-TCCACACTGTGAACCTCATCA-3′	5′-ACAGTGAGGGACAGCAAGATG-3′
G	5′-GTTGCTTCCGGTGTTGTTTTA-3′	5′-GTCTTGCTGCCGGGTTATAGT-3′
H	5′-ACTGCACGTTCAGGACATAGC-3′	5′-GCGTCGTCTTGTTGTAACCAT-3′
J1	5′-AGTCCACCACCCACACTGTAA-3′	5′-CTGACTACCATAGCCGTGCAT-3′
J2	5′-GTACTGACGTCATGCCCAAGT-3′	5′-CAGCTCTTCTGTTGCCATCTC-3′
J3	5′-TGGCTCCAAGTGTACTGGTTC-3′	5′-GGCATTATTGAAAAGCACGAA-3′
L	5′-ATACGATTAGCGGAGCAGGAT-3′	5′-AGTACAACGCCTGTGATGGTC-3′
M	5′-ATGGTAGAGCCCAACGGTAAA-3′	5′-AGCCAAACTTGAGGGAACACT-3′
N	5′-ACGCGAGCGACTACAAAGATA-3′	5′-TGTGTTGCTTACGCTGACAAG-3′
O	5′-TGTCCTGAAGTGCCTAACTGG-3′	5′-GATCTGACCTCTGCCTGACTG-3′
P	5′-GTTCGTGCTTGTTTTCATGGT-3′	5′-ATAGCCGTTCAGGAGATGCTT-3′
Q	5′-ATATACAGTCAGCGCCTGGTG-3′	5′-CCATCTTCATGTGGAGCAGTT-3′
R	5′-TGGATCAGGAATGGACTGATG-3′	5′-TAGCCTTTGTTGTGGTTGTCC-3′
GAPDH	5′-TCCACTGGAGTCTTCACAACC-3′	5′-TGCAGGTCCTTGGTGTACTTC-3′

(http://www.cbs.dtu.dk/services/SignalP/), and transmembrane sites were predicted from ApAChR-A using SMART analysis (http://smart.embl-heidelberg.de/). The alignment was used to create a tree with the neighbor joining method using Clustalx 2.1 (http://www.clustal.org/) (Saitou and Nei 1987). Positions with gaps were excluded by bootstrap resampling up to 1,000 trials and a random number generator seed of 111. Bootstrap labels were placed on nodes and saved as a Philip tree for observation using Treeview 1.6.6 (http://taxonomy.zoology.gla.ac.uk/rod/treeview.html). The tree was rooted with the *Aplysia* $GABA_A$ receptor α-subunit (GenBank accession no. AF322878) as an out-group and compared the ApAChRs with the following human nicotinic receptor subunits: α1 (NM_001039523), α2 (NM_000742), α3 (NM_000743), α4 (NM_000744), α5 (NM_000745), α6 (NM_004198), α7 (NM_000746), α9 (NM_017581), α10 (NM_020402), β1 (NM_000747), β2 (NM_000748), β3 (NM_000749), β4 (NM_000750), δ (NM_000751), γ (NM_005199), and ε (NM_000080). Identity values between human and *Aplysia* subunits, as well as the *Aplysia* acetylcholine binding protein (accession no. NM_001204559), were calculated using the pairwise alignment program from Jalview.

Analysis. The Clampfit analysis program of pCLAMP was used to determine the amplitude of changes to membrane potential or holding current evoked by neurotransmitters and drugs under current or voltage clamp. After at least 1 min of baseline, two cursors were placed immediately prior to the current or voltage change, while an additional two cursors were similarly positioned at the peak response. Clampfit then calculated the average current or voltage between the paired cursors. The maximal amplitude of the response was taken as the difference between these average baseline and peak values. Current was normalized to cell size by dividing by whole cell capacitance (as provided by the EPC-8 slow capacitance compensation circuitry). For display only, most current and voltage traces were filtered off-line to between 20 and 80 Hz using the Clampfit Gaussian filter. The slow nature of the responses ensured this second filtering brought about no change in amplitude or kinetics. Conductance was derived using Ohm's law ($G = I/V$) and the current change during a 200-ms step from -60 to -70 mV. In cases where nicotine was applied twice, the second application occurred ~10 min after the first. The peak current of the second response was then expressed as a percentage of the first response.

For intracellular Ca^{2+}, EasyRatioPro files were exported as .txt files and plotted as line graphs using Prism (version 3; GraphPad Software, La Jolla, CA). Analysis compared the steady-state value of the baseline 340/380 ratio with the ratio from a peak or new steady-state during agonist application. Averages of the baseline and new regions were determined by eye, if an obvious peak was present, or with adjacent averaging. Change was the difference between the new and the baseline ratio.

Relative expression levels of ApAChR subunits were taken from real-time PCR data by normalizing to the expression of ApGAPDH, as done by van Nierop et al. (2005, 2006) for LnAChR subunits. ΔCt was calculated as the Ct of a given ApAChR minus the Ct of ApGAPDH. This was transformed by raising the base of 2 to the negative ΔCt of each ApAChR and was then plotted in Prism.

Data are means ± SE. Statistical analysis was performed using Prism. The Kolmogorov-Smirnov method was used to test data sets for normality. To test whether the mean differed between two groups, either Student's paired or unpaired *t*-test (for normally distributed data) or the Mann-Whitney *U*-test (for not normally distributed data) was used. For three or more means, normally distributed data were compared using a standard one-way analysis of variance (ANOVA) followed by the Dunnett or Tukey-Kramer multiple comparisons test, whereas not normally distributed data were compared using the Kruskal-Wallis ANOVA and Dunn's multiple comparisons test. Means were considered significantly different if the two-tailed *P* value was <0.05.

RESULTS

Nicotinic agonists depolarize cultured bag cell neurons. In cultured bag cell neurons under sharp-electrode current clamp, a 2-s pressure application of 1 mM acetylcholine induced a response that either depolarized the cell, which then recovered toward resting potential (Fig. 1*A*), or activated a burst of action potentials (Fig. 1*B*). In 16 neurons, the average depolarization from -60 mV was ~35 mV (Fig. 1*F*), with 6 neurons firing action potentials. Considering that a strong depolarization will provoke voltage-gated Ca^{2+} influx and potentially activate nonselective cation channels (Gardam and Magoski 2009; Hung and Magoski 2007; Lupinsky and Magoski 2006; Tam et al. 2009), it was not surprising to find that three of the neurons reached a new steady state of -53.6 ± 1.5 mV. On the other hand, a 2-s pressure application of 3 mM nicotine stimulated the neurons much less, with an average depolarization of ~18 mV ($n = 15$) that was significantly different from depolarization by acetylcholine (Fig. 1*F*), and induced action potentials in only 3 of 15 neurons (Fig. 1*D*). We also assessed TMA, which activates nicotinic receptors via the same quaternary ammonium ion motif as acetylcholine (Ascher et al. 1978; Schmitt et al. 1999). At a level between nicotine and acetylcholine, the TMA-induced depolarization was ~24 mV ($n = 9$) (Fig. 1*E*), which was significantly different from that induced by acetylcholine, but not nicotine (Fig. 1*F*), with spiking observed in just 1 of the 9 neurons.

Nicotine produces a concentration-dependent inward current by opening an ionotropic receptor. We sought to obtain evidence for nicotine activating a receptor different from that of acetylcholine. Initially, cultured bag cell neurons were whole cell voltage-clamped at -60 mV in nASW with standard K-aspartate-containing intracellular solution and were given 10-s microperfusion applications of 3 mM nicotine repeated every 10 min. Unlike the acetylcholine response, which we previously showed desensitizes with repeated doses (White and Magoski 2012), nicotine failed to desensitize at the concentration and application times involved. To generate a dose response, multiple concentrations of nicotine (30 μM–10 mM) were delivered. Although 10 mM was always applied, not all doses were given to every neuron because of the finite time for which one is able to hold a cell. Examples of responses to 100 μM, 300 μM, 1 mM, and 3 mM nicotine are shown in Fig. 2*A*. When normalized to the initial maximal current at 10 mM, the resulting dose-response curve had a cooperative Hill value of 2.4 and an EC_{50} of 543 μM (Fig. 2*B*). Our prior work found acetylcholine to have a noncooperative Hill value of 0.7 and a smaller EC_{50} of 267 μM (White and Magoski 2012).

The current evoked by nicotine involved channel opening. Bag cell neurons were voltage-clamped at -60 mV and given several 200-ms steps to -70 mV (Fig. 2*C*, *bottom*). Initially, two of these steps were delivered as control, separated by 1–2 min, followed by a third step 2 min later at the peak of the response to a 10-s perfusion of 3 mM nicotine (concentration from the top of the curve). With the use of Ohm's law, conductance was calculated from the magnitude of the current produced by the step. The change in conductance during baseline conditions was determined by comparing the first and second control step currents. The conductance change due to nicotine was determined by comparing the second control step current and the acetylcholine step current. For display, leak

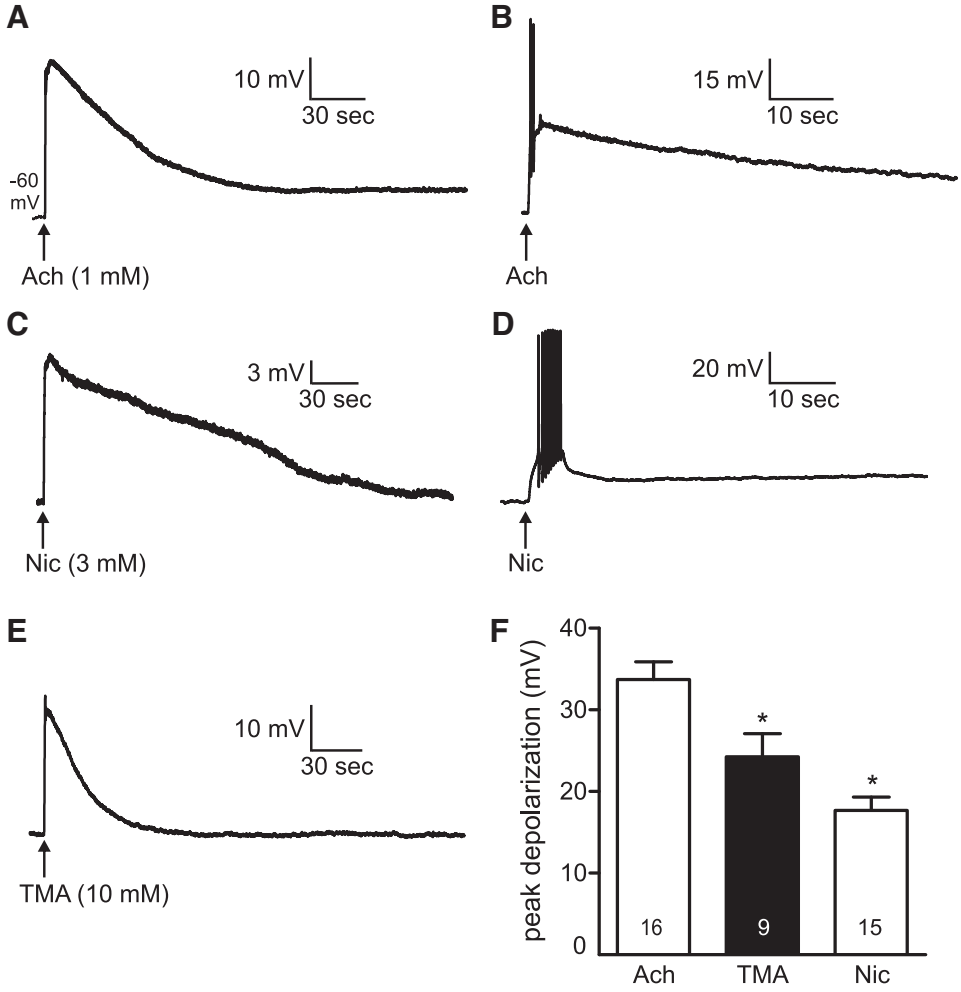

Fig. 1. Depolarization of cultured bag cell neurons by nicotinic agonists. *A*: under sharp-electrode current clamp, a 2-s pressure application of 1 mM acetylcholine (ACh) depolarized a cultured bag cell neuron in normal artificial seawater (nASW) from a resting potential of −60 mV. *B*: in 6 of 16 neurons, the depolarization was sufficient to reach action potential threshold. Values are means ± SE. *C*: nicotine at 3 mM also depolarized bag cell neurons, although to a lesser extent than ACh. *D*: nicotine delivery resulted in action potentials in only 3 of 15 neurons. *E*: the quaternary ammonium salt tetramethylammonium chloride (TMA) also depolarized bag cell neurons, to a degree between that of ACh and nicotine. *F*: summary graph indicating the average depolarization for ACh was significantly different from that for either TMA (*$P < 0.01$) or nicotine (*$P < 0.001$, ANOVA with Tukey-Kramer multiple comparisons test). Nic, nicotine; numbers in bars indicate number of neurons.

was removed from both the second control step current and the acetylcholine step current by subtracting the appropriate prior step current. Compared with control (Fig. 2*C*, *top*, black), there was an increase in conductance with nicotine ($n = 11$) (Fig. 2*C*, *top*, gray). The control change in conductance, taken 2 min before application of nicotine, revealed only a slight increase of ~3%, which was significantly different from the ~100% change in nicotine (Fig. 2*E*, *left*).

The nicotine response did not appear to involve metabotropic receptors. Cultured bag cell neurons were dialyzed under whole cell voltage clamp at −60 mV for 30 min with standard intracellular solution, where the normal 0.1 mM GTP was replaced with 10 mM GDPβS, a nonhydrolyzable form of GDP (Eckstein et al. 1979). Compared with parallel controls dialyzed with GTP ($n = 6$), introduction of GDPβS did not alter the peak current to pressure-applied 3 mM nicotine ($n = 5$) (Fig. 2*D*, gray vs. black), and the averaged data fail to show a significant difference (Fig. 2*E*, *right*). We and others have employed GDPβS to block G protein-coupled receptor-dependent responses in both *Aplysia* and *Lymnaea* neurons (Kehoe 1994; Lemos and Levitan 1984; Magoski et al. 1995; Tam et al. 2011; White and Magoski 2012).

Pharmacology of the nicotinic response. Given both a Hill value of 2.4 for nicotine vs. 0.7 for acetylcholine and the lack of desensitization to repeated nicotine applications, it appears that nicotine may gate a different receptor than acetylcholine. To explore this further, classic nicotinic antagonists were tested on the nicotine current in cultured bag cell neurons whole cell voltage-clamped at −60 mV. Nicotine (3 mM) was pressure-applied twice, for 2 s, with a minimum of 10 min between deliveries. Antagonists were introduced into the bath after the first nicotine application, and the relative effectiveness of the blocker was determined by the percent remaining peak current evoked during the second nicotine application.

Under control conditions, the nicotine response did not desensitize, i.e., when no antagonist was delivered, the second application of nicotine elicited a peak current that was essentially equal (~100%) to the first current ($n = 34$) (Fig. 3, *A* and *D*). We previously established that acetylcholine readily desensitizes and evoked a second current of just 55% of the first (White and Magoski, 2012). Several antagonist proved effective on the nicotine-induced response. The noncompetitive cholinergic blocker mecamylamine (100 μM) (Stone et al. 1956), reduced the second current to ~60% of the first ($n = 16$) (Fig. 3, *B* and *D*). This was a less robust block compared with acetylcholine, where our prior observation was that mecamylamine nearly eliminated the acetylcholine current (White and Magoski 2012). The general competitive antagonist dihydro-β-erythroidine (500 μM) (Folkers and Major 1937), inhibited the second nicotine current to a level ~40% of the first ($n = 6$) (Fig. 3, *B* and *D*). However, dihydro-β-erythroidine did not block the acetylcholine response [control %re-

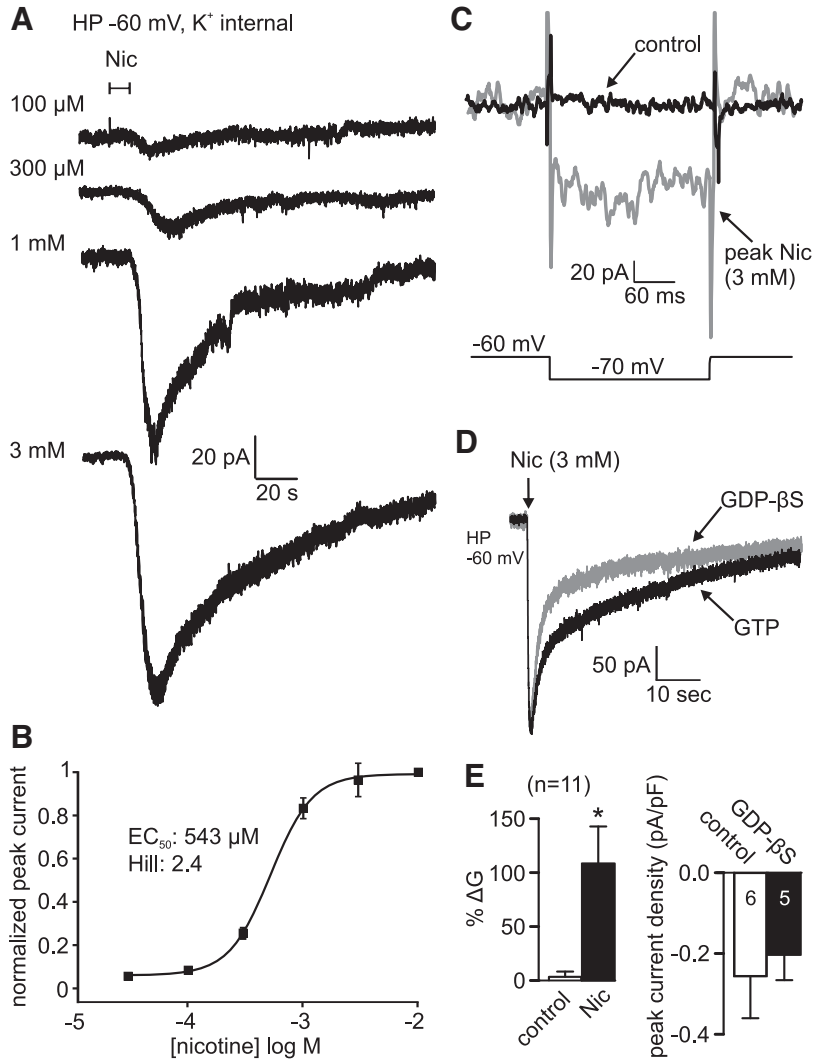

Fig. 2. Current responses to nicotine application in cultured bag cell neurons. *A*: under whole cell voltage clamp at −60 mV, 10-s applications of 0.1, 0.3, 1, and 3 mM nicotine perfused close to a bag cell neuron elicited inward currents of increasing magnitude. HP, holding potential. *B*: when the current was normalized to 10 mM, the fit of the dose-response curve provided a Hill value of 2.4 and an EC_{50} of 543 μM. Each neuron saw the largest dose first, with some or all of the subsequent doses delivered at an interval of ~10 min. *C*: leak-subtracted currents taken 1 min apart under voltage clamp during a 10-mV hyperpolarizing step (*bottom*). Before the addition of nicotine, essentially no conductance change occurred (black); however, a subtraction current taken at the peak of the 3 mM nicotine response presents an increase in conductance (gray). *D*: under voltage clamp at −60 mV, pressure application of 3 mM nicotine induced similar inward currents in cultured bag cell neurons dialyzed for 30 min with standard intracellular solution containing either 1 mM GTP (black) or 10 mM guanosine 5′-[β-thio]diphosphate trilithium salt (GDPβS; gray). The apparent difference in the decay kinetics of the nicotine-evoked current between GTP and GDPβS simply reflects variance in the data and is not significant (GTP: τ = 105.1 ± 35.2 s vs. GDPβS: τ = 102.9 ± 71.7 s; $P > 0.05$, Mann-Whitney *U*-test). *E*, *left*: summary data showing the percent change in conductance (%ΔG) between control and nicotine was significantly different (*$P < 0.05$, paired Student's *t*-test). *Right*, summary data indicate no significant difference between the peak current density induced by nicotine as a result of replacing GTP with GDPβS ($P > 0.05$, Mann-Whitney *U*-test). Values are means ± SE; numbers in bars indicate number of neurons.

maining peak current: 54.7 ± 3.5% (n = 26) vs. dihydro-β-erythroidine %remaining current: 49.7 ± 5.3% (n = 7); $P > 0.05$, unpaired Student's *t*-test]. Considering that strychnine blocks both the bag cell neuron afterdischarge and the acetylcholine current (Kaczmarek et al. 1978; White and Magoski 2012), as well as other *Aplysia* cholinergic synapses (Kehoe 1972), we examined its effect on the nicotine response and observed the second current to be ~60% of the first (n = 9) (Fig. 3, *C* and *D*). Finally, the nicotine current was not altered by either the competitive antagonist α-conotoxin ImI (1 μM; n = 11) (Paton and Zaimis 1948) or the noncompetitive antagonist hexamethonium (100 μM; n = 6) (McIntosh et al. 1994), as well as methyllycaconitine (1 μM; n = 8), a potential selective α7-receptor blocker (Alkondon et al. 1992; Ward et al. 1990) (Fig. 3*D*). Our past work showed both α-conotoxin ImI and hexamethonium strongly reduce the acetylcholine-elicited current in bag cell neurons (White and Magoski 2012).

The unpigmented small neurons from *Aplysia* right pleural ganglion present inward current in response to both acetylcholine and the quaternary ammonium ion motif-containing agonists TMA and DMPP (Ascher et al. 1978; Kehoe and McIntosh, 1998). When the latter two were tested on bag cell neurons, they evoked responses that were distinct in magnitude and comparable to acetylcholine and nicotine, respectively. Under whole cell voltage clamp at −60 mV, application of 10 mM TMA (n = 4), the simplest quaternary agonist (Burn and Dale 1915), produced a large current that at peak was similar in density to that elicited by 1 mM acetylcholine (n = 13) (Fig. 4, *A*, *B*, *E*). However, 10 mM DMPP (n = 9), a quaternary piperazine (Chen et al. 1951), and 3 mM nicotine (n = 8), both of which contain an aromatic ring, each provoked a 10-fold smaller response compared with acetylcholine or TMA (Fig. 4, *C*, *D*, *E*).

Ca^{2+} dependence of the acetylcholine and nicotine responses. Another factor that could distinguish between potentially disparate acetylcholine and nicotine receptors is Ca^{2+} permeability. Ionotropic acetylcholine receptors vary widely in the ability to pass Ca^{2+}; for example, α7-receptors conduct Ca^{2+} much more readily than other nicotinic receptors (Castro and Albuquerque 1995). We replaced extracellular Ca^{2+} with Mg^{2+} and observed changes in the reversal potential of the bag cell neuron acetylcholine and nicotine responses. For these experiments, Cs^+ was substituted for K^+ in the recording pipette to remove any potential confounding influence from voltage-gated K^+ currents. In initial tests, intracellular Cs^+ did not alter the reversal potential of the current brought about by pressure- or perfusion-applied 1 mM acetylcholine [−15.9 ± 1.4 mV for Cs^+ (n = 13) vs. −16.1 ± 1.9 mV for K^+ (n =

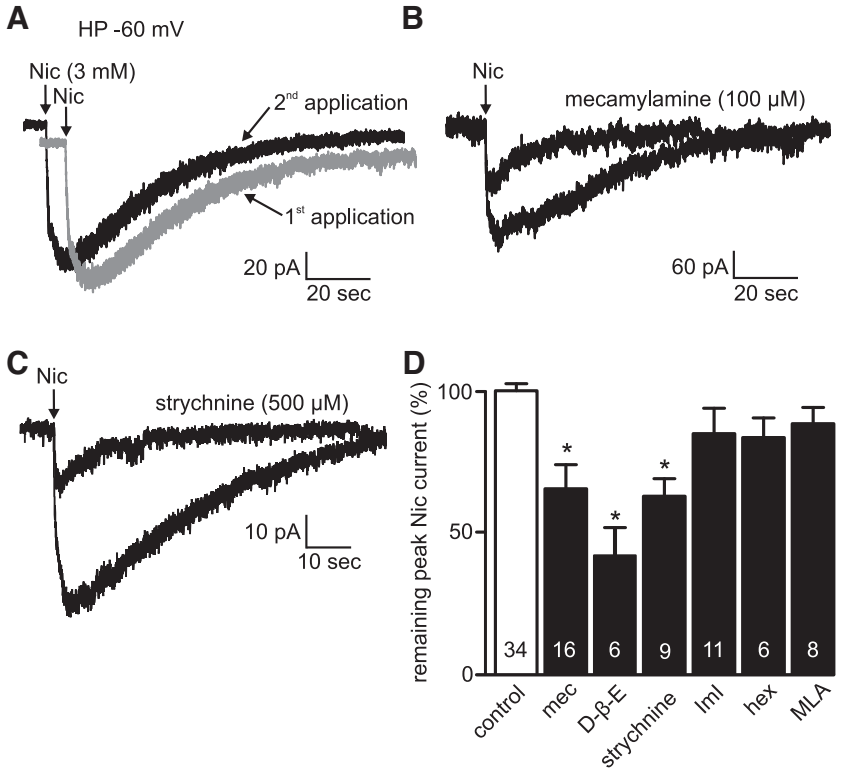

Fig. 3. Antagonist profile for the nicotine-induced current. *A*: in cultured bag cell neurons whole cell voltage-clamped at −60 mV, successive 2-s pressure applications of 3 mM nicotine, separated by ~10 min, produced similar currents with essentially no desensitization. The peak magnitude seen with the second application (black) was equal to that evoked by the first (gray; offset for clarity). *B*: the classic nicotinic antagonist mecamylamine blocked the nicotine-induced current. *C*: strychnine, a cholinergic blocker in molluscs, also reduced the second current. *D*: summary data showing the second nicotine application as a percentage of the first. Compared with control, 100 μM mecamylamine (mec), 500 μM dihydro-β-erythroidine (D-β-E), and 500 μM strychnine each significantly reduced the nicotine current, whereas 100 μM hexamethonium (hex), 1 μM α-conotoxin ImI (ImI), and 1 μM methyllycaconitine (MLA) had no effect ($P < 0.05$, Kruskal-Wallis ANOVA, Dunn's multiple comparisons test). Values are means ± SE; numbers in bars indicate number of neurons.

10); $P > 0.05$, unpaired Student's *t*-test]. To observe the reversal potential of acetylcholine- or nicotine-induced currents, a 6-s ramp from −60 to 0 mV was delivered during the peak of the response to a 10-s perfusion of agonist and, to eliminate leak currents, subtracted from a prior control ramp. Figure 5*A* shows currents comparing the reversal potential of the acetylcholine-evoked current in nASW and Ca^{2+}-free conditions. For acetylcholine, the reversal potential in Ca^{2+}-free ASW ($n = 9$) was not significantly different from nASW ($n = 13$), with both being ~18 mV (Fig. 5*C*). However, for the nicotine-induced current there was a significant, 6-mV leftward shift in the current-voltage curve from approximately −24 mV in nASW ($n = 16$) to approximately −30 mV in the absence of Ca^{2+} ($n = 9$) (Fig. 5, *B* and *C*). Also, a comparison of reversal potentials in nASW showed a significant difference between the more depolarized reversal for acetylcholine and the more hyperpolarized reversal for nicotine (Fig. 5*C*).

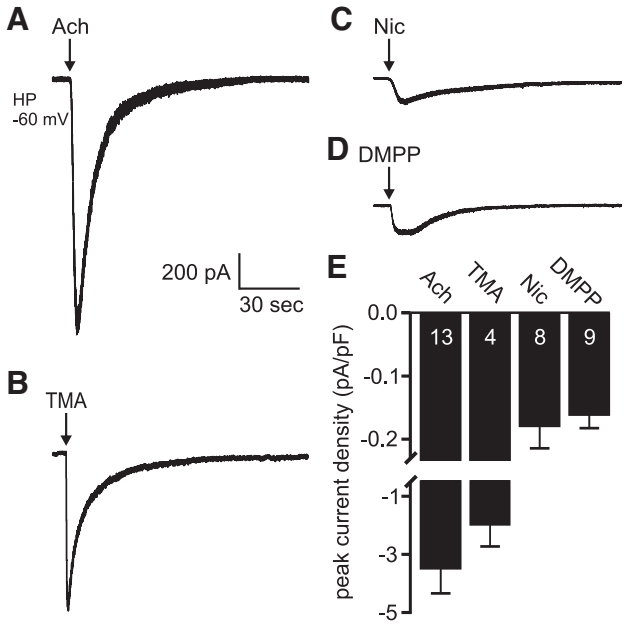

Fig. 4. Quaternary ammonium-based agonists exhibit differential potency. Examples are currents from cultured bag cell neurons induced by 2-s pressure applications of different nicotinic agonists held at −60 mV under whole cell voltage clamp: 1 mM ACh (*A*), 10 mM TMA (*B*), 3 mM nicotine (*C*), and 10 mM 1,1-dimethyl-4-phenylpiperazinium iodide (DMPP; *D*). *E*: summary data indicating that the average peak current density induced by TMA was similar to that provoked by acetylcholine. Conversely, DMPP resulted in a far smaller current density that was near to the response elicited by nicotine. Values are means ± SE; numbers in bars indicate number of neurons.

Our earlier work (White and Magoski 2012) demonstrated that block of the acetylcholine response by α-conotoxin ImI left behind a small current at −60 mV in nASW, also shown here in Fig. 5*D*. To confirm that this remaining current was not mediated by the α-conotoxin ImI-insensitive nicotine response, we examined the reversal potential at the peak of the response to 1 mM acetylcholine in the presence of 1 μM α-conotoxin ImI ($n = 6$). This remaining current presented an average reversal potential of approximately −17 mV and was not significantly different from that for acetylcholine alone in nASW (Fig. 5, *C* and *E*). There is also the prospect that, under control conditions, our 10-s perfusion or 2-s pressure applications of acetylcholine did in fact activate the nicotine receptor, but this portion of the response desensitized too quickly to be resolved. This was tested by pressure-applying 1 mM acetylcholine for 100 ms very close to bag cell neurons voltage-clamped at different potentials while perfusing with a fast-flowing stream of nASW (>1 ml/min; $n = 5$). This resulted in a rapid-onset current that

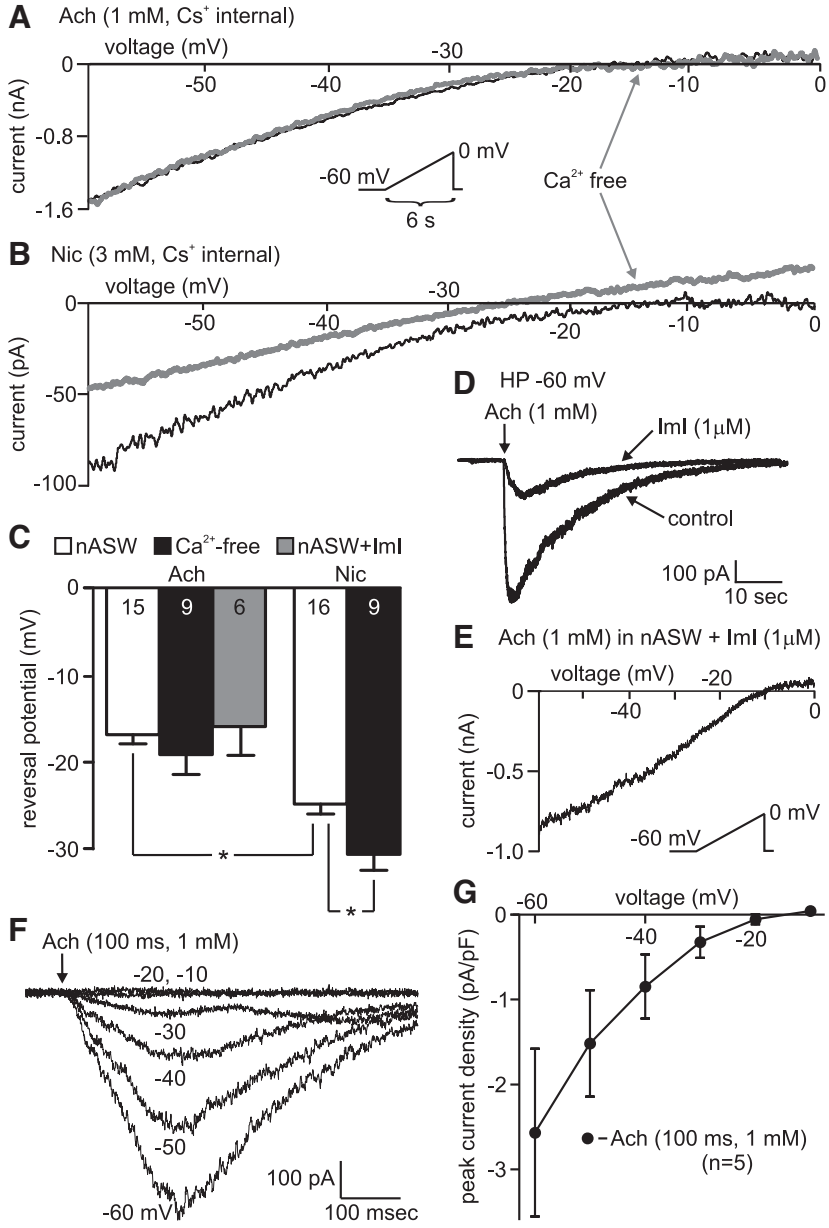

Fig. 5. The reversal potential of the nicotine- but not the ACh-induced current is sensitive to extracellular Ca^{2+}. *A*: leak-subtracted currents from separate cultured bag cell neurons under whole cell voltage clamp with Cs^{+}-based intracellular saline. There was no difference in the reversal potential in nASW (black) vs. Ca^{2+}-free medium (gray) of currents elicited by a 6-s ramp from −60 to 0 mV at the peak of the response to microperfused 1 mM ACh. *B*: when the same ramp was applied at the peak of the 3 mM nicotine response, a leftward shift of the reversal potential was observed in Ca^{2+}-free external compared with nASW. *C*: summary graph indicating no significant difference between the reversal potential of the acetylcholine-induced current in nASW alone vs. Ca^{2+}-free seawater and the current remaining in nASW after block by 1 μM α-conotoxin ImI ($P > 0.05$, KW-ANOVA, Dunn's multiple comparisons test). However, there was a significant change in the reversal potential of the nicotine current in Ca^{2+}-free seawater vs. nASW (*$P < 0.05$, Mann-Whitney *U*-test). The reversal potentials for nicotine and acetylcholine in nASW were also significantly different (*$P < 0.01$, unpaired Student's *t*-test). Values are means ± SE; numbers in bars indicate number of neurons. *D*: whole cell voltage-clamp recordings in nASW from the same neuron held at −60 mV show that the current produced by a 2-s pressure application of 1 mM ACh was diminished with the subsequent introduction of 1 μM α-conotoxin ImI. *E*: a subtraction current evoked in nASW by a ramp from −60 to 0 mV at the peak of the residual response to 1 mM ACh in the presence of 1 μM α-conotoxin ImI. *F*: pressure application of 1 mM ACh for 100 ms in close proximity to the soma of a cultured bag cell neuron in a stream of nASW. A fast, inward current was evoked by the ACh that decreased in magnitude as the steady-state holding potential was changed from −60 to −10 mV. *G*: the mean peak current density of the fast ACh current at different voltages provided a reversal potential of approximately −15 mV.

reversed at approximately −15 mV (Fig. 5, *F* and *G*), which is very similar to that resolved using the voltage ramp and 10 s of acetylcholine perfusion.

The Ca^{2+} sensitivity of the nicotine current reversal potential suggests that the channel(s) responsible pass Ca^{2+}. To bolster this, we added 1 mM of the Ca^{2+}-imaging dye fura PE3 (Geiger et al. 2009; Kachoei et al. 2006; Vorndran et al. 1995) to the intracellular solution while excluding both EGTA and Ca^{2+}. After the neurons were fura-loaded with 10 min of whole-cell dialysis under voltage clamp at −60 mV, a 2-s pressure application of 1 mM acetylcholine ($n = 13$) induced a rapid, large inward current (Fig. 6*A*, *bottom*) but no measureable increase in the 340/380 ratio (Fig. 6*A*, *top*). In contrast, pressure application of 3 mM nicotine ($n = 11$) evoked a much smaller current (Fig. 6*B*, *bottom*) yet elevated intracellular Ca^{2+} (Fig. 6*B*, *top*). The average density of the peak acetylcholine current (approximately −2.5 pA/pF) was significantly different from that of nicotine (~0.1 pA/pF; Fig. 6*C*); nonetheless, nicotine caused a significantly larger Ca^{2+} rise, based on an increase in the 340/380 ratio (Fig. 6*D*).

Identification of potential nicotinic-type receptor subunits in Aplysia. If nicotine and acetylcholine gate distinct receptors, one may expect *Aplysia* to have multiple ionotropic acetylcholine receptors genes. However, prior to the present study, only two nicotinic receptors had been published in GenBank: an *Aplysia* α1-subunit (accession no. AF467898) and an *Aplysia* non-α-subunit (accession no. AAL37250). Yet, van Nierop et al. (2006) reported 12 nicotinic receptors in the related pond snail, *Lymnaea* (LnAChR-A through -L). Hence, we searched the University of California, Santa Cruz *Aplysia* genome using BLAT and Prot2Gene with LnAChR protein sequences as input. This produced predicted sequences for 12 *Aplysia* AChR subunits, which we named ApAChR-A through ApAChR-L, based on their similarity to the *Lymnaea* receptors (van Nierop et al. 2006). Subsequently, nine more receptors were found and, to continue the convention, designated ApAChR-J2 and J3

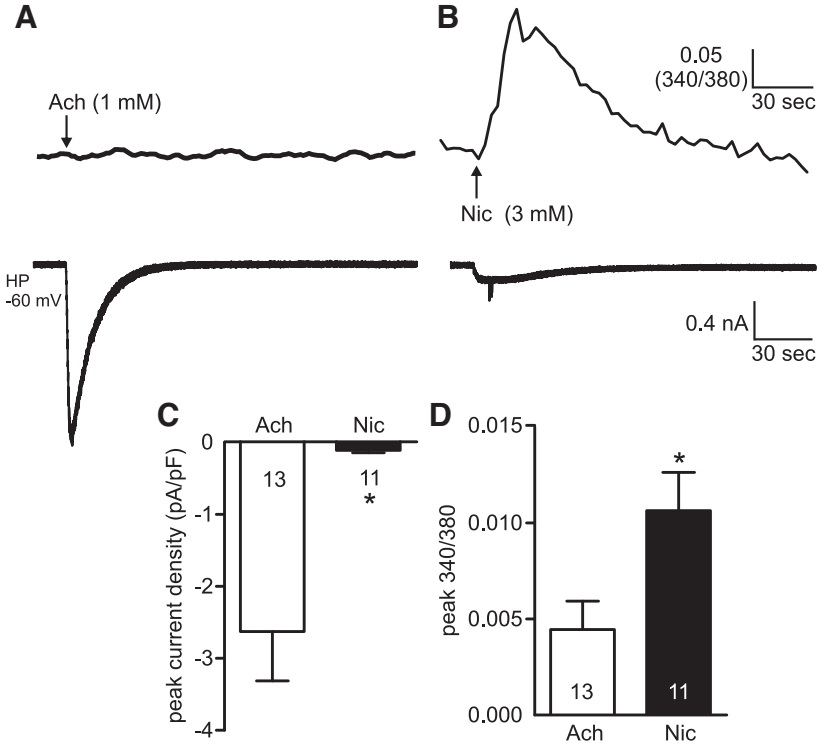

Fig. 6. Nicotine, but not ACh, induces an increase in intracellular Ca^{2+}. Simultaneous measurement of free intracellular Ca^{2+}, using fura PE3 fluorescence, and agonist-induced current under whole cell voltage clamp at −60 mV in cultured bag cell neurons. *A*: after a 2-s pressure application of 1 mM ACh, which induced a large rapid current (*bottom*), no observable change was apparent in the intensity of the 340/380 fluorescence ratio (*top*). *B*: conversely, application of 3 mM nicotine elicited a relatively small inward current and a simultaneous rise in intracellular Ca^{2+}. *C*: summary data indicating a significantly smaller current density produced by nicotine compared with ACh (*$P < 0.0001$, Mann-Whitney *U*-test). *D*: summary data showing an average increase in the 340/380 fluorescence ratio due to the nicotine-evoked current that was significantly different from that due to ACh (*$P < 0.05$, Mann-Whitney *U*-test). Values are means ± SE; numbers in bars indicate number of neurons.

(similar to ApAChR-J1), K2 (similar to ApAChR-K1), as well as M, N, O, P, Q, and R. With the exception of ApAChR-N, these additional subunits were first identified in a *Lymnaea* CNS transcriptome shotgun assembly as LnAChRs (Sadamoto et al. 2012) and then found via BLAST searches of an *Aplysia* RNA sequence assembly transcriptome from the Institute of Genome Sciences, University of Maryland.

After in silico sequences had been achieved for all 21 subunits, 16 were identified as putative cation-selective ApAChRs on the basis of an absence of the conserved Pro and Ala that line the pore adjacent to the second transmembrane domain of anion-selective cys-loop receptors (Galzi et al. 1992; Jensen et al. 2005). PCR was used to achieve overlapping full-length open reading frames for the putative cation-selective receptors: ApAChR-A, C, D, E, G, H, J1, J2, J3, L, M, N, O, P, Q, and R. See Table 1 for primers against noncoding 5′- and 3′-untranslated regions as well as internal coding regions. ApAChR-E is nearly identical to the published *Aplysia* α1-receptor (only a 4-amino acid difference), whereas ApAChR-J1 is identical to the *Aplysia* non-α-receptor. Those five ApAChRs predicted to be anion selective, i.e., ApAChR-B, F, I, K1, and K2, were not pursued further.

Comparing the *Aplysia* protein sequences with the archetypical muscle nicotinic receptor α1-subunit from *Torpedo californica* (GenBank accession no. P02710) indicated that all putative cation-selective ApAChRs possess amino acid similarities to nicotinic receptors in the cys-loop ligand-gated channel superfamily, specifically, an extracellular NH_2-terminal binding domain with two highly conserved Cys residues (corresponding to Cys128 and Cys142 in *Torpedo*), six agonist binding loops (loops A–F), a membrane-spanning region containing the ion conduction pore, four conserved transmembrane domains (M1–M4), and a variable intracellular loop between M3 and M4 (Unwin 1998).

Based on the presence of vicinal Cys192 and Cys193 (*Torpedo* numbering) (Kao et al. 1984; Sine, 2002), potential α-receptors are ApAChR-A, C, D, E, G, H, L, M, N, O, P, and R (aligned in Fig. 7). Conversely, a lack of vicinal Cys suggests ApAChR-J1, J2, J3, and Q are candidate β-receptors. Among the α-receptors, ApAChR-A, C, E, G, and N contain all four highly conserved aromatic amino acids (Tyr93, Trp149, Tyr190, and Tyr198 in *Torpedo*) in loops A, B, and C of the principal component of the agonist binding pocket (Arias 2000). The binding pockets of ApAChR-D, M, P, and R have Phe substituted for Tyr at *Torpedo* equivalent Y198. Akk et al. (1999) reported that this swapping of aromatic residues in the *Torpedo* receptor does not affect binding and moderately impacts gating. However, ApAChR-H has Tyr substituted for Trp at corresponding W149 in *Torpedo*, which may well alter binding, given that this residue interacts with acetylcholine (Arias 2000; Zhong et al. 1998). ApAChR-L is unlikely to possess full agonist-binding potential, because of a charged His substituted for Tyr in loop A at *Torpedo* equivalent Y93; similarly, loop C of ApAChR-O has a nonpolar Ser and a His residue at *Torpedo* equivalent Y190 and Y198, respectively, suggesting it may be an accessory subunit.

Phylogeny and relative expression of Aplysia nicotinic receptors. A radial tree was created using the putative cation-selective ApAChRs and the equivalent LnAChRs, with the exceptions of LnAChR-N, which we were unable to find, and LnAChR-P, the sequence of which was too short. For this comparison, neither the amino termini nor the highly variable regions between M3 and M4 were included. The resulting hypothesis of relationship suggested that the ApAChRs appeared to have diverged from a common ancestor in three separate clades, with ApAChR-A and N arising on their own,

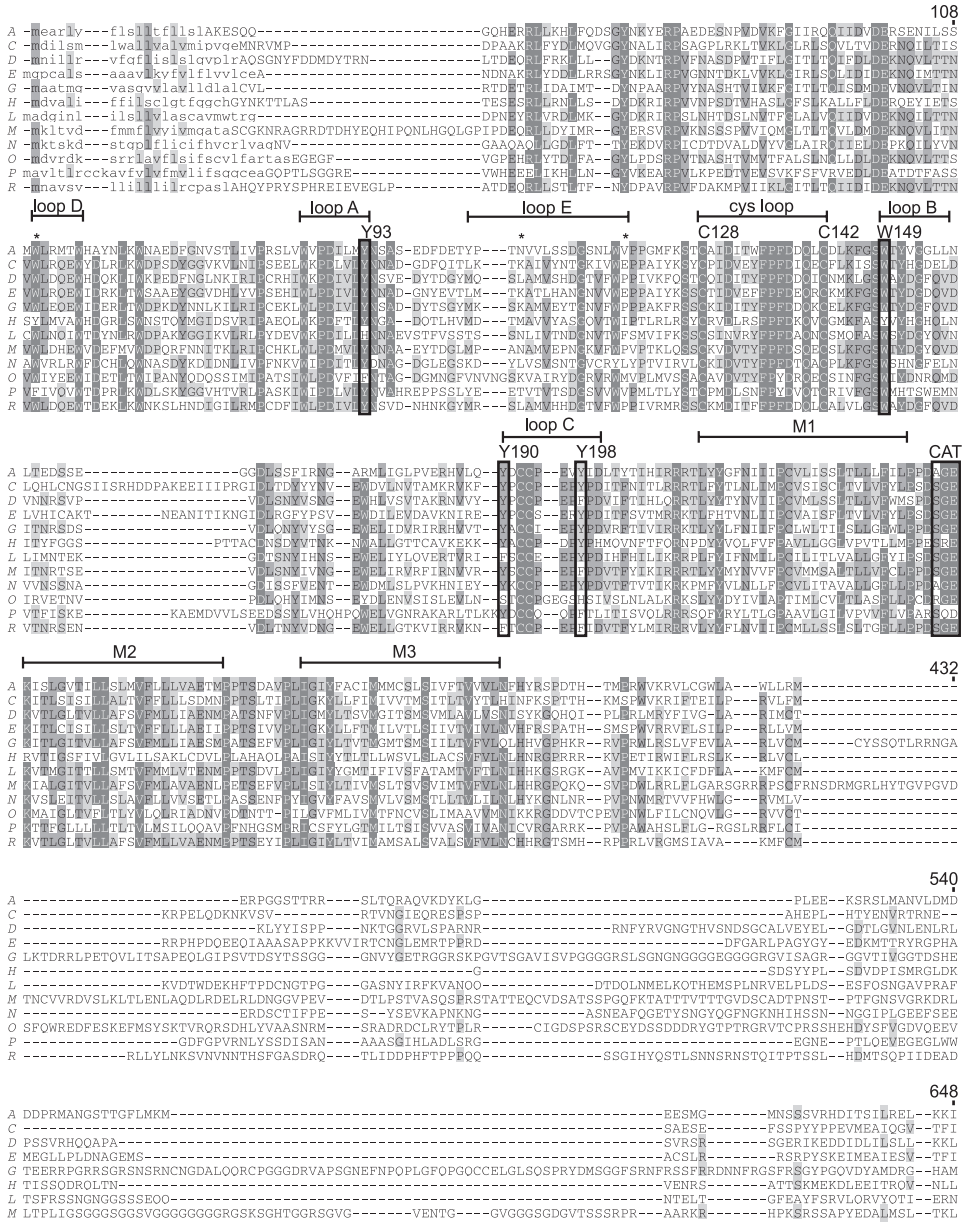

Fig. 7. Protein sequence alignment for putative cation selective nicotinic ACh receptor subunits of *Aplysia* (ApAChRs) using multiple sequence comparison by log-expectation (MUSCLE). Amino acids conserved in all ApAChRs are highlighted in dark gray, those moderately conserved in medium gray, and residues in the minority in light gray. The NH_2-terminal signal peptide for each subunit is shown in lower case. Based on analysis of ApAChR-A, the cys-loop, loops A–C of the principle binding component, loops D and E of the complementary binding component, and the 4 transmembrane domains (M1–M4) are labeled. The aromatic amino acids involved with ligand binding are numbered as per the sequence of the α1 nicotinic receptor from *Torpedo* and are surrounded by boxes for clarity, including the conserved region required for cation permeability (CAT). Residues that contribute to loops D and E of the complementary binding domain are indicated by asterisks.

ApAChR-C, E, J1, J2, and J3 as one group, and ApAChR-D, G, H, L, M, O, P, Q, and R as another group (Fig. 8*A*). Of course, such analysis does not provide the complete history and can only imply what may have happened during evolution.

We next used the *Aplysia* $GABA_A$ receptor as an out-group to root a second tree comparing *Aplysia* and human receptor subunits (Fig. 8*B*). This suggested many ApAChRs could have diverged from a common ancestor before the evolution of the human homomeric α7, α9, and α10, with ApAChR-H and P possibly being the oldest. The *Aplysia* subunits closest to human nicotinic receptors are ApAChR-E, sharing 51 and 47% sequence identity with α2 and α3, respectively, and ApAChR-C, being 42 and 43% identical to α2 and α3 (Table 3). Despite an overall highest similarity with α2, ApAChR-J1, J2, and J3 possess homologous amino acids in loops D and E of the complementary binding domain (Arias 2000; Sine 2002), and not surprisingly, their next closest homologs are β2 and β4.

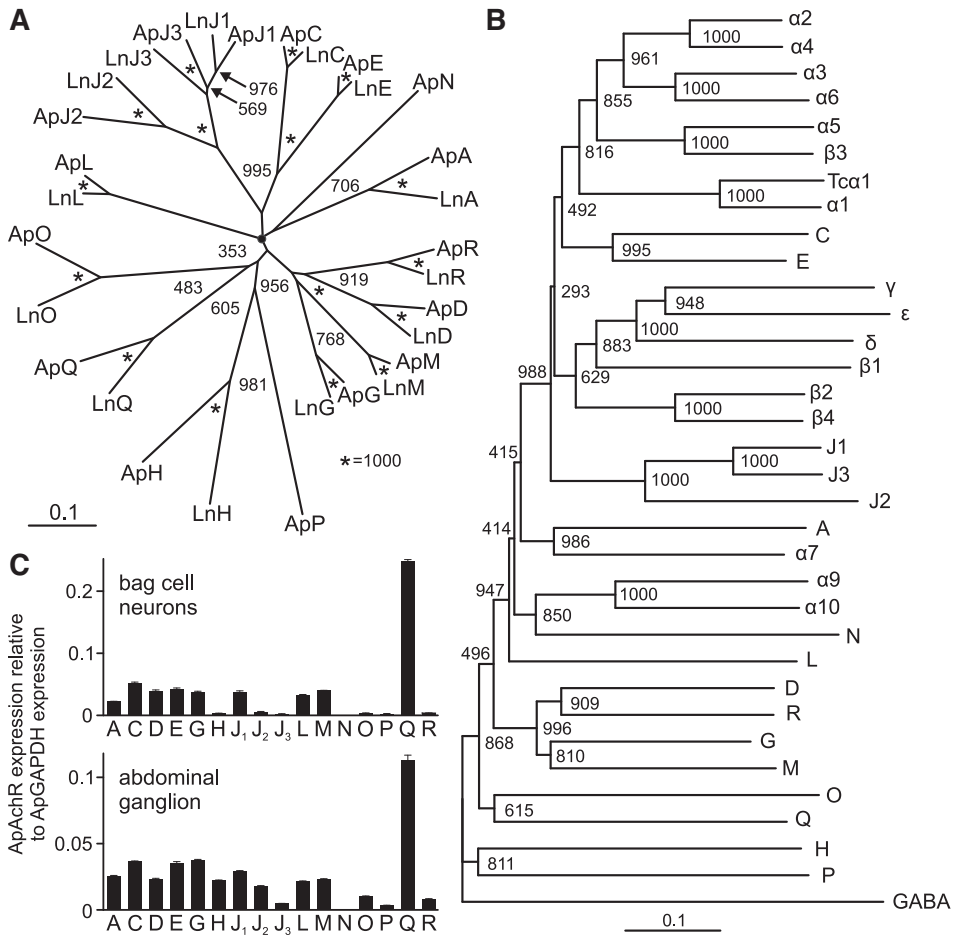

Fig. 8. Phylogenetic tree and real-time PCR of *Aplysia* nicotinic receptor subunits. *A*: radial tree of putative cation-selective ACh receptors from *Aplysia* and *Lymnaea* using the neighbor-joining clustering algorithm, excluding the amino termini and the regions between M3 and M4. Bootstrap numbers placed on nodes are based on 1,000 replicates (asterisk = 1,000 iterations), with the scale bar representing substitutions per site. From a common node of origin (black dot in center), the hypothesis of relationship implies that the receptors split into one (ApAChR-C, E, J1, J2, J3), two (ApAChR-D, G, H, L, M, O, P, Q, R), and three (ApAChR-A and N) distinct clades. *B*: tree of the ApAChRs and human nicotinic receptors rooted with the *Aplysia* $GABA_A$ receptor as an out-group and bootstrap values. The majority of ApAChRs appear to have emerged before α7, α9, and α10, although ApAChR-J1, J2, and J3 could have a shared origin with most of the β-receptors and other accessory subunits. Finally, there may be a mutual origin for ApAChR-C and E with the remaining α-receptors and *Torpedo* α1. *C*: relative expression levels of ApAChRs in bag cell neuron cluster (*top*) and abdominal ganglion (*bottom*). Summary data represent real-time PCR of ApAChR expression levels relative to the housekeeping gene, ApGAPDH, with cDNA template derived from 3 separate pairs of bag cell neuron clusters or 3 separate abdominal ganglia (sans the bag cell neurons). ApAChR-Q appears to have the highest expression in both the bag cell neurons and the abdominal ganglion, with ApAChR-A, C, D, E, G, J1, L, and M likely at similar levels. The bag cell neurons seem to have less expression of ApAChR-H, J2, J3, O, P, and R, which is also the case for the abdominal ganglion, with the exception of slightly greater amounts of ApAChR-J2, O, and R. Both regions expressed very little, if any, of the ApAChR-N subunit.

To gain an indication of which ApAChR subunits are potentially expressed in tissues of interest, real-time PCR was performed using cDNA from either bag cell neuron clusters or abdominal ganglion (sans the bag cell neuron clusters) and normalized to the *Aplysia* housekeeping gene GAPDH. A similar undertaking was made by van Nierop et al. (2005, 2006) for LnAChR in different regions of the *Lymnaea* CNS. Interestingly, ApAChR-Q had the highest relative expression in the bag cell neurons, despite the sequence data suggesting it would not contribute to agonist binding. The next highest relative expression was the α-like ApAChR-C, followed by ApAChR-A, D, E, G, L, and M to a roughly equal degree, along with the β-like ApAChR-J1 (Fig. 8*C*, *top*). There was limited relative expression of ApAChR-H, J2, J3, O, P, and R, as well as a very small amount of ApAChR-N. For the abdominal ganglion, the relative expression of ApAChR-Q was again the greatest, with ApAChR-A, C, D, E, G, H, J1, J2, L, and M all present to a lesser extent, whereas ApAChR-J3, P, and R were the least expressed, and ApAChR-N, like the bag cell neurons, was almost absent (Fig. 8*C*, *bottom*). Note that during the PCR of full-length sequences using the primers in Table 1, the band intensities of the various subunit products provided qualitatively similar results, with ApAChR-N being consistently amplified in very low amounts. This stated, the apparent levels of relative expression of multiple genes could be influenced by differences in primer pair efficiency and ultimately must be considered an estimate.

dsRNA targeting of select Aplysia receptor subunits reduces the acetylcholine or nicotine current. We attempted to knock down subunits contributing to the acetylcholine- or nicotine-induced currents. ApAChR-C and E were selected as candidates for the acetylcholine receptor given that they should possess full binding potential for acetylcholine, are present in relatively high amounts in bag cell neurons, and appear most

Table 3. *Pairwise amino acid identity of Aplysia nicotinic receptor subunits with human nicotinic receptor subunits*

	AChBP	α1	α2	α3	α4	α5	α6	α7	α9	α10	β1	β2	β3	β4	δ	γ	E
A	28	34	39	38	37	33	37	**43**	32	35	31	36	33	35	32	32	30
C	28	38	42	**44**	38	37	41	36	34	36	35	39	38	40	36	32	32
D	30	30	32	33	31	33	32	34	34	**34**	28	33	30	30	29	28	28
E	27	38	**51**	47	42	42	45	37	37	36	37	46	44	46	36	33	33
G	29	34	36	34	33	34	34	34	35	**37**	29	33	33	32	31	29	29
H	26	24	26	28	27	25	25	27	26	**28**	27	24	25	26	23	24	23
J1	24	33	**41**	40	37	34	38	36	31	32	34	38	35	39	33	31	29
J2	24	31	31	32	30	**34**	32	30	25	28	28	31	34	33	30	28	29
J3	23	35	**41**	40	36	35	38	33	31	33	35	39	36	39	36	30	30
L	27	32	33	34	32	**36**	34	35	32	34	32	31	32	33	31	30	25
M	29	31	33	31	29	32	**43**	35	32	34	33	30	32	29	30	28	27
N	26	30	30	32	30	30	33	35	35	**36**	29	29	30	30	29	28	25
O	23	26	28	26	27	28	26	25	28	**28**	27	25	29	27	24	24	25
P	26	24	27	26	25	21	27	26	26	**28**	24	25	27	25	27	23	25
Q	24	30	28	28	26	29	28	29	31	**31**	27	25	30	27	27	28	28
R	32	30	34	32	32	34	30	32	31	**35**	30	29	32	31	28	28	28

Percent sequence identity of aligned ApAChR and human AChR subunits, as well as the *Aplysia* acetylcholine binding protein (AChBP). Bold numbers reflect the highest scores.

closely related to the prototypical α3 group (see Fig. 8, *B* and *C*). Conversely, ApAChR-H and P were chosen as candidates for the nicotine receptor because they appear to be the oldest, are some of the least abundant subunits, and lack a Trp at *Torpedo* equivalent W55 (see asterisk under loop D label in Fig. 7). Loss of this Trp more severely impairs gating by acetylcholine than by nicotine (Corringer et al. 1998; Xie and Cohen 2001).

Initially, we incubated cultured bag cell neurons for 3–4 days in 600 ng/ml dsRNA directed against ApAChR-C or E. As a control, neurons were treated with 600 ng/ml dsRNA corresponding to the untranslated region of the newt retinoic receptor (which has no significant sequence similarity to any known *Aplysia* transcripts). Compared with control ($n = 5$), exposure to ApAChR-C or E dsRNA ($n = 6$ and 6) produced no change in the peak current density evoked by a 2-s pressure application of 1 mM acetylcholine under whole cell voltage clamp at −60 mV (Fig. 9*C*). However, including dsRNA for both ApAChR-C and E (300 ng/ml each; $n = 14$) did reduce the acetylcholine-elicited current by ~50% compared with control ($n = 14$) (Fig. 9, *A* and *D*). Yet, the combination of dsRNA for ApAChR-C and E did not change the current in response to pressure-applied 3 mM nicotine ($n = 11$) relative to control ($n = 5$) (Fig. 9*E*). Conversely, treating neurons with both ApAChR-H and P dsRNA (300 ng/ml each; $n = 10$) attenuated the nicotine-evoked current, again by more than 50% in contrast with control ($n = 7$) (Fig. 9, *B* and *F*), whereas the response to acetylcholine was the same in neurons subjected to the ApAChR-H and P dsRNA cocktail ($n = 6$) and control cells ($n = 10$) (Fig. 9*G*).

DISCUSSION

Ionotropic cholinergic receptors typically bind nicotine with high affinity and acetylcholine with low affinity, the latter thought to be necessary for high-frequency input (Hurst et al. 2012). However, we find that in bag cell neurons, nicotine appears to trigger a separate receptor from acetylcholine. Whereas there are ionotropic receptors that are acetylcholine sensitive and nicotine insensitive, the reverse has not been previously reported, and we believe our data is novel in suggesting separate acetylcholine- and nicotine-activated receptors. First, the current gated by nicotine, but not acetylcholine, is blocked by the competitive antagonist dihydro-β-erythroidine. Conversely, a different competitive antagonist, α-conotoxin ImI, as well as the noncompetitive antagonist hexamethonium, exclusively attenuates the acetylcholine-evoked current. Second, DMPP imitates the current elicited by nicotine, whereas the acetylcholine response is mimicked by TMA, which contains an ammonium ion motif, like acetylcholine, and may bind in a similar manner (Lape et al. 2009). Third, Ca^{2+} removal left-shifts the nicotine current reversal potential and nicotine elevates intracellular Ca^{2+}, suggesting the nicotine receptor is Ca^{2+} permeable. Meanwhile, the acetylcholine current reversal potential is not altered by Ca^{2+}-free saline and acetylcholine does not change intracellular Ca^{2+}, consistent with this receptor not passing Ca^{2+}. Fourth, the two responses present differential sensitivity to dsRNA exposure, with the targeting of ApAChR-H and P reducing the nicotine-evoked current and that of ApAChR-C and E lessening the current produced by acetylcholine.

In addition to presenting different pharmacology and Ca^{2+} permeability, the nicotine current is also smaller in magnitude, more cooperative, and desensitizes less compared with acetylcholine. Thus nicotine may activate a different receptor subtype with a different binding pocket. The highly conserved aromatic amino acids in the principal component of the ligand-binding site are responsible for affinity, whereas the more variable complementary component mediates selectivity (Albuquerque et al. 2009). Differences in certain residues on the principle subunits could reduce affinity or agonist-induced channel activation such that the receptor is selective for one agonist over the other (Arias 2000). Alternatively, if there are changes to key residues of the complementary subunits, this may result in the loss of selectivity for a particular agonist. A cholinergic ionotropic receptor failing to respond to nicotine is not unprecedented; for example, nicotine does not gate either the α9 or α9/10 nicotinic receptor (Elgoyhen et al. 1994, 2001). In the bag cell neurons, it is possible that nicotine evokes a smaller response because of a partial agonist effect on the acetylcholine receptor, as seen with the chicken α3β2

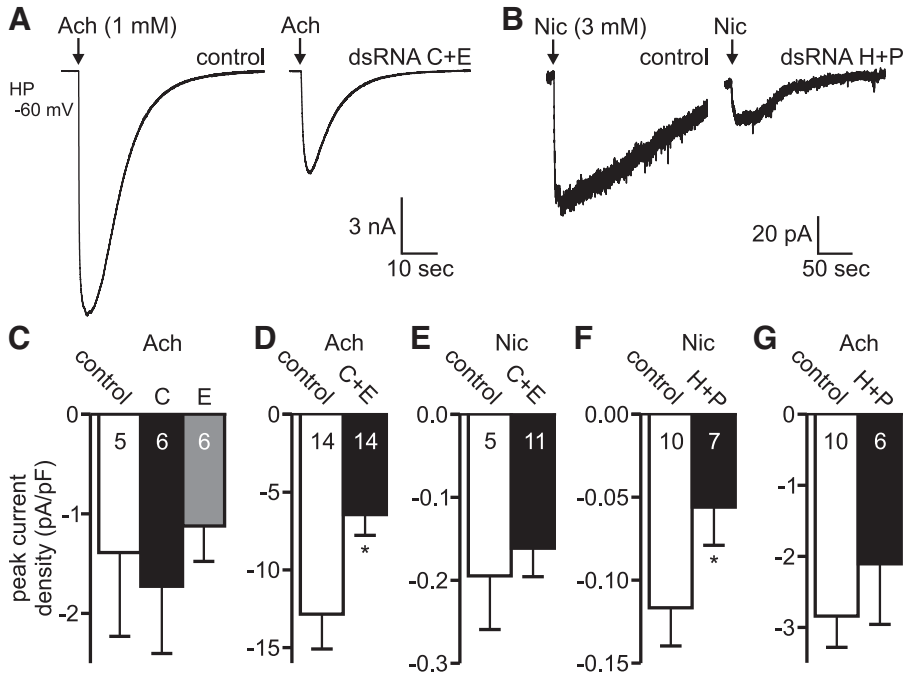

Fig. 9. Double-stranded RNA (dsRNA) targeting of the ACh and nicotine currents. *A*, *left*: after incubation in 600 ng/ml dsRNA corresponding to the 5′-untranslated region of the newt retinoic acid receptor (acting as a control), a 2-s pressure application of 1 mM ACh generated a large inward current in a cultured bag cell neuron whole cell voltage-clamped to −60 mV. *Right*, the magnitude of the acetylcholine-induced current was reduced by half after culturing in 300 ng/ml dsRNA ApAChR-C and 300 ng/ml dsRNA ApAChR-E (C+E). *B*, *left*: subsequent to control dsRNA treatment, delivery of 3 mM nicotine elicited a typical inward current at −60 mV. *Right*, culturing in 300 ng/ml dsRNA of both ApAChR-H and ApAChR-P (H+P) attenuated the nicotine-evoked current. *C–G*: summary data of the peak current density for the ACh or nicotine responses after treatment with different dsRNAs. The ordinate label applies to all graphs. *C*: there was no significant difference in the current brought about by ACh between control and neurons incubated in either ApAChR-C or E dsRNA alone ($P > 0.05$, ANOVA, Dunnett multiple comparison test). *D*: however, the ACh-induced current was significantly different after culturing in a cocktail of ApAChR-C + E dsRNA (*$P < 0.05$, unpaired Student's *t*-test). *E*: the same ApAChR-C + E dsRNA treatment did not significantly alter the response to nicotine ($P > 0.05$, unpaired Student's *t*-test). *F*: instead, compared with control, the current elicited by nicotine was rendered significantly smaller following incubation in 300 ng/ml each of ApAChR-H + P dsRNA (*$P < 0.05$, Mann-Whitney *U*-test). *G*: this combination of ApAChR-H + P dsRNA did not result in a significant difference for the ACh-elicited current compared with control (unpaired Student's *t*-test). Values are means ± SE; numbers in bars indicate number of neurons.

receptor (Hussy et al. 1994). This may occur through lower-affinity nicotine binding, failure to trigger full opening, or nicotine acting as a pore blocker (Kuryatov et al. 2000; Paradiso and Steinbach 2003; Rush et al. 2002). For NMDA receptors, low-affinity agonists produce currents that decay more quickly and recover from desensitization faster (Lester and Jahr 1992). However, these alternative mechanisms would likely not give rise to the differential block of the bag cell neuron nicotine and acetylcholine currents by dihydro-β-erythroidine and α-conotoxin ImI/hexamethonium, respectively. The cation-selective, but not the chloride-selective, acetylcholine receptor from *Aplysia* buccal and pleural neurons is also exclusively sensitive to conotoxin ImI/hexamethonium (Kehoe and McIntosh 1998).

Differences between the magnitude and desensitization of the acetylcholine- and nicotine-gated currents do not necessarily distinguish between two receptors. For example, the single-channel conductance of human α7-receptors is different when opened by acetylcholine compared with an allosteric agonist (Pałczyńska et al. 2012). Yet, conductance is not a function of the agonist for cholinergic currents from unpigmented right pleural *Aplysia* neurons (Ascher et al. 1978), a mouse muscle-like cell line (Papke et al. 1988), and rat α4/β2 receptors (Akk and Auerbach 1999). In bag cell neurons, if both acetylcholine and nicotine were acting on the same channel, one would not expect nicotine to exclusively increase intracellular Ca^{2+} or the nicotine-induced current to have a more negative reversal potential and be sensitive to Ca^{2+} removal. Similarly, it is probably not the case that the larger acetylcholine response masks a nicotine component, given that the acetylcholine-elicited current remaining after α-conotoxin ImI presented the same reversal potential as acetylcholine alone. We also failed to uncover evidence that the nicotine receptor opens but then quickly desensitizes during acetylcholine delivery. Brief pressure application of acetylcholine under fast-flowing perfusion results in a rapid-onset current that reverses at a voltage similar to the other acetylcholine responses, but not at a voltage like the nicotine response or a combination of the two responses. Thus the possibility of two distinct receptors appears plausible.

The large number of ApAChR subunits present in bag cell neurons is enigmatic, since there are only two distinct currents. The *Aplysia* transcriptome contains at least 20 acetylcholine receptors, 16 of which could be excitatory, based on the sequence of the conserved M1–M2 linker involved in ion permeability (Sine and Engel 2006). Each subunit may have a specialized role in transmission, depending on agonist sensitivity, gating kinetics, permeability, and desensitization. The seemingly high expression of ApAChR-Q is equally puzzling, considering that the lack of conserved amino acids in the binding pocket implies it likely does not bind acetylcholine. Its function could be structural, as is the case for the α5, β1, and β3 receptor subunits, which are thought to occupy the non-

binding fifth position in certain cholinergic receptors (Arias 2000). Alternatively, ApAChR-Q could have a nonsynaptic role, such as receptor trafficking and assembly, like the vertebrate α5-subunit (Ramirez-Latorre et al. 1996), or represent a chemotaxic sensor, similar to channels found in *Caenorhabditis* chemosensory neurons (Yassin et al. 2001) and certain prokaryotes (Tasneem et al. 2005).

The major cholinergic receptor in vertebrate autonomic ganglion is the heteromeric, α-conotoxin ImI-sensitive $\alpha3\beta2/\beta4$ (Conroy and Berg 1995; Listerud et al. 1991; Ramirez-Latorre et al. 1996). Nicotine itself activates vertebrate α7 (Anand et al. 1993), the LnAChR-A homolog in *Lymnaea* (van Nierop et al. 2005), and the anionic-selective α7-like receptor in *Aplysia* (Kehoe and McIntosh 1998). Block of the bag cell neuron acetylcholine-induced current by α-conotoxin ImI suggests either an α7- or $\alpha3\beta2$-type receptor (Ellison et al. 2004; Johnson et al. 1995). However, the lack of activation by nicotine and the failure of MLA to reduce the current rules against α7. The possibility of a $\alpha3\beta2$-type heteromeric receptor is strengthened by the homology of $\alpha2/\alpha3$ to the higher-expressing ApAChR-C and E, as well as the knockdown of the acetylcholine current by combined ApAChR-C and E dsRNA treatment. Assuming the nicotine response is mediated by a distinct receptor, the dsRNA experiments would suggest ApAChR-C or E are not involved, but rather ApAChR-H and P may contribute to the channel gated by nicotine. Consistent with this, the absence of a key Trp in complementary loop D (*Torpedo* equivalent W55) of both ApAChR-H and P would likely impair acetylcholine binding (Corringer et al. 1998; Xie and Cohen 2001). The remaining subunits either are more likely to be acetylcholine sensitive (ApAChR-A and G), possess an altered binding pocket (ApAChR-D, L, M, O, and R), or are probably not present in significant enough abundance (ApAChR-N). These speculations are based on pharmacology and a limited application of dsRNA technology. Definitive proof would require heterologous expression of multiple combinations of ApAChR subunits and subsequent physiological characterization. Unfortunately, attempts at expressing invertebrate receptors in oocytes or cell lines have seen limited success. In fact, the only *Lymnaea* cation-selective receptor that has been expressed is LnAChR-A, and it is both acetylcholine and nicotine activated (van Nierop et al. 2005).

If there are two separate receptors in bag cell neurons, it begs the question, what is the endogenous agonist for the nicotine receptor? Like *Aplysia*, many other cloned invertebrate cys-loop receptors possess differences in binding pocket amino acids and may respond to other transmitters (Barbara et al. 2008; Dent 2006; Tricoire-Leignel and Thany 2010). With the exception of acetylcholine, all classical neurotransmitters either inhibit or do not change the bag cell neuron membrane potential (Kaczmarek et al. 1978; Whim and Kaczmarek 1998; White and Magoski 2012). Thus, if there is an endogenous agonist for the nicotinic receptor, it may be a peptide, perhaps related to certain bungarotoxin-like peptides (Tsetlin 1999), or a metabolite (Grando 2008; Yassin et al. 2001). Because the putative nicotine receptor is Ca^{2+} permeable, it would allow for Ca^{2+} influx at voltages nearer to the resting membrane potential than that permitted by voltage-gated Ca^{2+} channels (Tam et al. 2009). For example, α7-receptors produce Ca^{2+} transients in dendritic spines, whereas α3-containing receptors augment global Ca^{2+} increases through Ca^{2+}-induced Ca^{2+}-release (Shoop et al. 2001). In addition, different states of receptor desensitization could confer a role in bag cell neuron plasticity; i.e., long after the acetylcholine response has desensitized, which presumably occurs during the afterdischarge, nicotine-gated channels could still be recruited to directly permit Ca^{2+} entry.

An alternative and intriguing prospect is that the separate acetylcholine and nicotine receptors are adaptive. Bourne et al. (2010) suggest the role of acetylcholine binding protein in *Aplysia* may be to buffer dinoflagellate toxins, such as red tide. By extension, the overwhelming prominence of acetylcholine-sensitive receptors in the bag cell neuron cholinergic response may serve as a defense against protists or predatory worms that have co-evolved nicotine-mimetic toxins (Kem 1997; Schwarz et al. 2003). The smaller-magnitude nicotinic response in bag cell neurons would be insufficient to permit toxin-mediated activation of reproduction. Because egg-laying behavior lowers the defenses of *Aplysia* (Goldsmith and Byrne 1993; Mackey and Carew 1983), this could protect the animal from predation.

ACKNOWLEDGMENTS

We thank S. L. Smith and H. M. Fuller-Hodgson for technical assistance, A. K. H. Tam for initial work on the acetylcholine current, and the anonymous reviewers for constructive criticism of the work.

GRANTS

S. H. White held a McLaughlin/Bracken and a Queen Elizabeth II Scholarship in Science Technology. N. S. Magoski held a Canadian Institutes of Health Research (CIHR) New Investigator Award. This work was supported by a CIHR operating grant (to N. S. Magoski).

DISCLOSURES

No conflicts of interest, financial or otherwise, are declared by the authors.

AUTHOR CONTRIBUTIONS

S.H.W., C.J.C., and N.S.M. conception and design of research; S.H.W. and C.J.C. performed experiments; S.H.W., C.J.C., and N.S.M. analyzed data; S.H.W., C.J.C., and N.S.M. interpreted results of experiments; S.H.W. and N.S.M. prepared figures; S.H.W. drafted manuscript; C.J.C. and N.S.M. edited and revised manuscript; N.S.M. approved final version of manuscript.

REFERENCES

Akk G, Auerbach A. Activation of muscle nicotinic acetylcholine receptor channels by nicotinic and muscarinic agonists. *Br J Pharmacol* 128: 1467–1476, 1999.

Akk G, Zhou M, Auerbach A. A mutational analysis of the acetylcholine receptor channel transmitter binding site. *Biophys J* 76: 207–218, 1999.

Albuquerque EX, Pereira EF, Alkondon M, Rogers SW. Mammalian nicotinic acetylcholine receptors: from structure to function. *Physiol Rev* 89: 73–120, 2009.

Alkondon M, Pereira EF, Wonnacott S, Albuquerque EX. Blockade of nicotinic currents in hippocampal-neurons defines methyllycaconitine as a potent and specific receptor antagonist. *Mol Pharmacol* 41: 802–808, 1992.

Anand R, Peng X, Ballesta JJ, Lindstrom J. Pharmacological characterization of alpha-bungarotoxin-sensitive acetylcholine receptors immunoisolated from chick retina: contrasting properties of alpha 7 and alpha 8 subunit-containing subtypes. *Mol Pharmacol* 44: 1046–1050, 1993.

Arch S. Polypeptide secretion from the isolated parietovisceral ganglion of *Aplysia californica*. *J Gen Physiol* 59: 47–59, 1972.

Arias HR. Localization of agonist and competitive antagonist binding sites on nicotinic acetylcholine receptors. *Neurochem Int* 36: 595–645, 2000.

Ascher P, Marty A, Neild TO. Life time and elementary conductance of channels mediating excitatory effects of acetylcholine in *Aplysia* neurons. *J Physiol* 278: 177–206, 1978.

Barbara GS, Grunewald B, Paute S, Gauthier M, Raymond-Delpech V. Study of nicotinic acetylcholine receptors on cultured antennal lobe neurones from adult honeybee brains. *Invert Neurosci* 8: 19–29, 2008.

Bhargava A, Dallman MF, Pearce D, Choi S. Long double-stranded RNA-mediated RNA interference as a tool to achieve site-specific silencing of hypothalamic neuropeptides. *Brain Res Protoc* 13: 115–125, 2004.

Bodmer R, Levitan I.B. Sensitivity of *Aplysia* neurons in primary culture to putative neurotransmitters. *J Neurobiol* 15: 429–440, 1984.

Bourne Y, Radic Z, Araoz R, Talley TT, Benoit E, Servent D, Taylor P, Molgo J, Marchot P. Structural determinants in phycotoxins and AChBP conferring high affinity binding and nicotinic AChR antagonism. *Proc Natl Acad Sci USA* 107: 6076–6081, 2010.

Burn JH, Dale HH. The action of certain quarternary ammonium bases. *J Pharmacol Exp Ther* 6: 417–438, 1915.

Castro NG, Albuquerque EX. Alpha-bungarotoxin-sensitive hippocampal nicotinic receptor channel has a high calcium permeability. *Biophys J* 68: 516–524, 1995.

Chen G, Portman R, Wickel A. Pharmacology of 1,1-dimethyl-4-phenylpiperazinium iodide, a ganglion stimulating agent. *J Pharmacol Exp Ther* 103: 330, 1951.

Chiu A, Hunkapiller MW, Heller E, Stuart DK, Hood LE, Strumwasser F. Purification and primary structure of the neuropeptide egg-laying hormone of *Aplysia californica*. *Proc Natl Acad Sci USA* 76: 6656–6660, 1979.

Conroy WG, Berg DK. Neurons can maintain multiple classes of nicotinic acetylcholine receptors distinguished by different subunit compositions. *J Biol Chem* 270: 4424–4431, 1995.

Corringer PJ, Bertrand S, Bohler S, Edelstein SJ, Changeux JP, Bertrand D. Critical elements determining diversity in agonist binding and desensitization of neuronal nicotinic acetylcholine receptors. *J Neurosci* 18: 648–657, 1998.

Corringer P.J, Baaden M, Bocquet N, Delarue M, Dufresne V, Nury H, Prevost M, Van Renterghem C. Atomic structure and dynamics of pentameric ligand-gated ion channels: new insight from bacterial homologues. *J Physiol* 588: 565–572, 2010.

Dent JA. Evidence for a diverse cys-loop ligand-gated ion channel superfamily in early bilateria. *J Mol Evol* 62: 523–535, 2006.

Dwoskin LP, Crooks PA. Competitive neuronal nicotinic receptor antagonists: a new direction for drug discovery. *J Pharmacol Exp Ther* 298: 395–402, 2001.

Eckstein F, Cassel D, Levkovitz H, Lowe M, Selinger Z. Guanosine 5′-*O*-(2-thiodiphosphate)-inhibitor of adenylate-cyclase stimulation by guanine-nucleotides and fluoride ions. *J Biol Chem* 254: 9829–9834, 1979.

Edgar RC. MUSCLE: multiple sequence alignment with high accuracy and high throughput. *Nucleic Acids Res* 32: 1792–1797, 2004.

Elgoyhen AB, Johnson DS, Boulter J, Vetter DE, Heinemann S. Alpha 9: an acetylcholine receptor with novel pharmacological properties expressed in rat cochlear hair cells. *Cell* 79: 705–771, 19945.

Elgoyhen AB, Vetter DE, Katz E, Rothlin CV, Heinemann SF, Boulter J. Alpha10: a determinant of nicotinic cholinergic receptor function in mammalian vestibular and cochlear mechanosensory hair cells. *Proc Natl Acad Sci USA* 98: 3501–3506, 2001.

Ellison M, Gao F, Wang HL, Sine SM, McIntosh JM, Olivera BM. Alpha-conotoxins ImI and ImII target distinct regions of the human alpha7 nicotinic acetylcholine receptor and distinguish human nicotinic receptor subtypes. *Biochemistry* 43: 16019–16026, 2004.

Ferguson GP, Ter Maat A, Parsons DW, Pinsker HM. Egg laying in *Aplysia*. I. Behavioral patterns and muscle activity of freely behaving animals after selectively elicited bag cell discharges. *J Comp Physiol A* 164: 835–847, 1989.

Fire A, Xu S, Montgomery MK, Kostas SA, Driver SE, Mello CC. Potent and specific genetic interference by double-stranded RNA in *Caenorhabditis elegans*. *Nature* 391: 806–811, 1998.

Fisher T, Lin CH, Kaczmarek LK. The peptide FMRFa terminates a discharge in *Aplysia* bag cell neurons by modulating calcium, potassium, and chloride conductances. *J Neurophysiol* 69: 2164–2173, 1993.

Folkers K, Major RT. Isolation of erythroidine, an alkaloid of curare action, from *Erythrina americana* Mill. *J Am Chem Soc* 59: 1850–1851, 1937.

Galzi JL, Devillers-Thiery A, Hussy N, Bertrand S, Changeux J.P, Bertrand D. Mutations in the channel domain of a neuronal nicotinic receptor convert ion selectivity from cationic to anionic. *Nature* 359: 500–505, 1992.

Gardam KE, Magoski NS. Regulation of cation channel voltage- and Ca^{2+}-dependence by multiple modulators. *J Neurophysiol* 102: 259–271, 2009.

Geiger JE, Hickey CM, Magoski NS. Ca^{2+} entry through a non-selective cation channel in *Aplysia* bag cell neurons. *Neuroscience* 162: 1023–1038, 2009.

Goldsmith JR, Byrne JH. Bag cell extract inhibits tail-siphon withdrawal reflex, suppresses long-term but not short-term sensitization, and attenuates sensory-to- motor neuron synapses in *Aplysia*. *J Neurosci* 13: 1688–1700, 1993.

Grando SA. Basic and clinical aspects of non neuronal acetylcholine: biological and clinical significance of non-canonical ligands of epithelial nicotinic acetylcholine receptors. *J Pharmacol Sci* 106: 174–179, 2008.

Hickey CM, Groten CJ, Sham L, Carter CJ, Magoski NS. Voltage-gated Ca^{2+} influx and mitochondrial Ca^{2+} initiate secretion from *Aplysia* neuroendocrine cells. *Neuroscience* 250: 755–772, 2013.

Hurst R, Rollema H, Bertrand D. Nicotinic acetylcholine receptors: from basic science to therapeutics. *Pharmacol Ther* 137: 22–54, 2013.

Hung AY, Magoski NS. Activity-dependent initiation of a prolonged depolarization in *Aplysia* bag cell neurons: role for a cation channel. *J Neurophysiol* 97: 2465–2479, 2007.

Hussy N, Ballivet M, Bertrand D. Agonist and antagonist effects of nicotine on chick neuronal nicotinic receptors are defined by alpha and beta subunits. *J Neurophysiol* 72: 1317–1326, 1994.

Jensen ML, Schousboe A, Ahring PK. Charge selectivity of the cys-loop family of ligand-gated ion channels. *J Neurochem* 92: 217–225, 2005.

Johnson DS, Martinez J, Elgoyhen AB, Heinemann SF, McIntosh JM. Alpha-conotoxin ImI exhibits subtype-specific nicotinic acetylcholine receptor blockade: preferential inhibition of homomeric alpha 7 and alpha 9 receptors. *Mol Pharmacol* 48: 194–199, 1995.

Jones AK, Sattelle DB. The cys-loop ligand-gated ion channel gene superfamily of the red flour beetle, *Tribolium castaneum*. *BMC Genomics* 8: 327, 2007.

Kachoei BA, Knox RJ, Uthuza D, Levy S, Kaczmarek LK, Magoski NS. A store-operated Ca^{2+} influx pathway in the bag cell neurons of *Aplysia*. *J Neurophysiol* 96: 2688–2698, 2006.

Kaczmarek LK, Jennings K, Strumwasser F. Neurotransmitter modulation, phosphodiesterase inhibitor effects, and cyclic AMP correlates of afterdischarge in peptidergic neurites. *Proc Natl Acad Sci USA* 75: 5200–5204, 1978.

Kao PN, Dwork AJ, Kaldany RR, Silver ML, Wideman J, Stein S, Karlin A. Identification of the alpha subunit half-cystine specifically labeled by an affinity reagent for the acetylcholine receptor binding site. *J Biol Chem* 259: 11662–11665, 1984.

Kauer JA, Kaczmarek LK. Peptidergic neurons of *Aplysia* lose their response to cyclic adenosine 3′:5′-monophosphate during a prolonged refractory period. *J Neurosci* 5: 1339–1345, 1985.

Kehoe J. Glutamate activates a K^+ conductance increase in *Aplysia* neurons that appears to be independent of G-proteins. *Neuron* 13: 691–702, 1994.

Kehoe J. Ionic mechanisms of a two-component cholinergic inhibition in *Aplysia* neurones. *J Physiol* 225: 85–114, 1972.

Kehoe J, McIntosh JM. Two distinct nicotinic receptors, one pharmacologically similar to the vertebrate alpha7-containing receptor, mediate Cl^- currents in *Aplysia* neurons. *J Neurosci* 18: 8198–8213, 1998.

Kehoe J, Buldakova S, Acher F, Dent J, Bregestovski P, Bradley J. *Aplysia* cys-loop glutamate-gated chloride channels reveal convergent evolution of ligand specificity. *J Mol Evol* 69: 125–141, 2009.

Kem WR. Alzheimer's drug design based upon an invertebrate toxin (anabaseine) which is a potent nicotinic receptor agonist. *Invert Neurosci* 3: 251–259, 1997.

Kupfermann I, Kandel ER. Electrophysiological properties and functional interconnections of two symmetrical neurosecretory clusters (bag cells) in abdominal ganglion of *Aplysia*. *J Neurophysiol* 33: 865–876, 1970.

Kuryatov A, Olale FA, Choi C, Lindstrom J. Acetylcholine receptor extracellular domain determines sensitivity to nicotine-induced inactivation. *Eur J Pharmacol* 393: 11–21, 2000.

Lape R, Krashia P, Colquhoun D, Sivilotti, LG. Agonist and blocking actions of choline and tetramethylammonium on human muscle acetylcholine receptors. *J Physiol* 587: 5045–5072, 2009.

Lee YS, Choi SL, Lee SH, Kim H, Park H, Lee N, Lee SH, Chae YS, Jang DJ, Kandel ER, Kaang BK. Identification of a serotonin receptor coupled to adenylyl cyclase involved in learning-related heterosynaptic facilitation in *Aplysia*. *Proc Natl Acad Sci USA* 106: 14634–14639, 2009.

Lemos JR, Levitan IB. Intracellular injection of guanyl nucleotides alters the serotonin-induced increase in potassium conductance in *Aplysia* neuron R15. *J Gen Physiol* 83: 269–285, 1984.

Lester RA, Jahr CE. NMDA channel behavior depends on agonist affinity. *J Neurosci* 12: 635–643, 1992.

Listerud M, Brussaard AB, Devay P, Colman DR, Role LW. Functional contribution of neuronal AChR subunits revealed by antisense oligonucleotides. *Science* 254: 1518–1521, 1991.

Lupinsky DA, Magoski NS. Ca^{2+}-dependent regulation of a non-selective cation channel from *Aplysia* bag cell neurones. *J Physiol* 575: 491–506, 2006.

Mackey S, Carew TJ. Locomotion in *Aplysia*: triggering by serotonin and modulation by bag cell extract. *J Neurosci* 3: 1469–1477, 1983.

Magoski NS, Bauce LG, Syed NI, Bulloch AG. Dopaminergic transmission between identified neurons from the mollusk, *Lymnaea stagnalis*. *J Neurophysiol* 74: 1287–1300, 1995.

McIntosh JM, Yoshikami D, Mahe E, Nielsen DB, Rivier JE, Gray WR, Olivera BM. A nicotinic acetylcholine-receptor ligand of unique specificity, alpha-conotoxin-ImI. *J Biol Chem* 269: 16733–16739, 1994.

Moroz LL, Edwards JR, Puthanveettil SV, Kohn AB, Ha T, Heyland A, Knudsen B, Sahni A, Yu F, Liu L, Jezzini S, Lovell P, Iannucculli W, Chen M, Nguyen T, Sheng H, Shaw R, Kalachikov S, Panchin YV, Farmerie W, Russo JJ, Ju J, Kandel ER. Neuronal transcriptome of *Aplysia*: neuronal compartments and circuitry. *Cell* 127: 1453–1467, 2006.

Norekian TP. GABAergic excitatory synapses and electrical coupling sustain prolonged discharges in the prey capture neural network of *Clione limacina*. *J Neurosci* 19: 1863–1875, 1999.

Papke RL, Millhauser G, Lieberman Z, Oswald RE. Relationships of agonist properties to the single channel kinetics of nicotinic acetylcholine receptors. *Biophys J* 53: 1–10, 1988.

Paradiso KG, Steinbach JH. Nicotine is highly effective at producing desensitization of rat alpha4beta2 neuronal nicotinic receptors. *J Physiol* 553: 857–871, 2003.

Paton WD and Zaimis EJ. Clinical potentialities of certain bisquaternary salts causing neuromuscular and ganglionic block. *Nature* 162: 810, 1948.

Pałczyńska MM, Jindrichova M, Gibb AJ, Millar NS. Activation of α7 nicotinic receptors by orthosteric and allosteric agonists: influence on single-channel kinetics and conductance. *Mol Pharmacol* 82: 910–917, 2012.

Ramirez-Latorre J, Yu CR, Qu X, Perin F, Karlin A, Role L. Functional contributions of alpha5 subunit to neuronal acetylcholine receptor channels. *Nature* 380: 347–351, 1996.

Richmond JE, Jorgensen EM. One GABA and two acetylcholine receptors function at the *C. elegans* neuromuscular junction. *Nat Neurosci* 2: 791–797, 1999.

Rothlin CV, Katz E, Verbitsky M, Elgoyhen AB. The alpha9 nicotinic acetylcholine receptor shares pharmacological properties with type A gamma-aminobutyric acid, glycine, and type 3 serotonin receptors. *Mol Pharmacol* 55: 248–254, 1999.

Rush R, Kuryatov A, Nelson ME, Lindstrom J. First and second transmembrane segments of alpha3, alpha4, beta2, and beta4 nicotinic acetylcholine receptor subunits influence the efficacy and potency of nicotine. *Mol Pharmacol* 61: 1416–1422, 2002.

Sadamoto H, Takahashi H, Okada T, Kenmoku H, Toyota M, Asakawa Y. De novo sequencing and transcriptome analysis of the central nervous system of mollusc *Lymnaea stagnalis* by deep RNA sequencing. *PLoS One* 7: e42546, 2012.

Saitou N, Nei M. The neighbor-joining method: a new method for reconstructing phylogenetic trees. *Mol Biol Evol* 4: 406–425, 1987.

Schmitt JD, Sharples CG, Caldwell WS. Molecular recognition in nicotinic acetylcholine receptors: the importance of pi-cation interactions. *J Med Chem* 42: 3066–3074, 1999.

Schwarz S, Kämpchen T, Tilotta MC, Gündisch D, Seitz G. Synthesis and nicotinic binding studies on enantiopure pinnamine variants with an 8-azabicyclo[3.2.1]octane moiety. *Pharmazie* 58: 295–299, 2003.

Shoop RD, Chang KT, Ellisman MH, Berg DK. Synaptically driven calcium transients via nicotinic receptors on somatic spines. *J Neurosci* 21: 771–781, 2001.

Sigvardt KA, Rothman BS, Brown RO, Mayeri E. The bag cells of *Aplysia* as a multitransmitter system: identification of alpha bag cell peptide as a second neurotransmitter. *J Neurosci* 6: 803–813, 1986.

Simmons LK, Koester J. Serotonin enhances the excitatory acetylcholine response in the RB cell cluster of *Aplysia californica*. *J Neurosci* 6: 774–781, 1986.

Sine SM. The nicotinic receptor ligand binding domain. *J Neurobiol* 53: 431–446, 2002.

Sine SM, Engel AG. Recent advances in cys-loop receptor structure and function. *Nature* 440: 448–455, 2006.

Stone CA, Torchiana ML, Navarro A, Beyer KH. Ganglionic blocking properties of 3-methylamino-isocamphane hydrochloride (mecamylamine)–a secondary amine. *J Pharmacol Exp Ther* 117: 169–183, 1956.

Tam AK, Geiger JE, Hung AY, Groten CJ, Magoski NS. Persistent Ca^{2+} current contributes to a prolonged depolarization in *Aplysia* bag cell neurons. *J Neurophysiol* 102: 3753–3765, 2009.

Tam AK, Gardam KE, Lamb S, Kachoei BA, Magoski NS. Role for protein kinase c in controlling *Aplysia* bag cell neuron excitability. *Neuroscience* 179: 41–55, 2011.

Tasneem A, Iyer LM, Jakobsson E, Aravind L. Identification of the prokaryotic ligand-gated ion channels and their implications for the mechanisms and origins of animal cys-loop ion channels. *Genome Biol* 6: R4, 2005.

Thompson AJ, Lester HA, Lummis SC. The structural basis of function in cys-loop receptors. *Q Rev Biophys* 43: 449–499, 2010.

Tricoire-Leignel H, Thany SH. Identification of critical elements determining toxins and insecticide affinity, ligand binding domains and channel properties. *Adv Exp Med Biol* 683: 45–52, 2010.

Tsetlin V. Snake venom α-neurotoxins and other 'three-finger' proteins. *Eur J Biochem* 264: 281–286, 1999.

Unwin N. The nicotinic acetylcholine receptor of the *Torpedo* electric ray. *J Struct Biol* 121: 181–190, 1998.

van Kesteren RE, Carter C, Dissel HM, van Minnen J, Gouwenberg Y, Syed NI, Spencer GE, Smit AB. Local synthesis of actin-binding protein beta-thymosin regulates neurite outgrowth. *J Neurosci* 26: 152–157, 2006.

van Nierop P, Keramidas A, Bertrand S, van Minnen J, Gouwenberg Y, Bertrand D, Smit AB. Identification of molluscan nicotinic acetylcholine receptor (nAChR) subunits involved in formation of cation- and anion-selective nAChRs. *J Neurosci* 25: 10617–10626, 2005.

van Nierop P, Bertrand S, Munno DW, Gouwenberg Y, van Minnen J, Spafford JD, Syed NI, Bertrand D, Smit AB. Identification and functional expression of a family of nicotinic acetylcholine receptor subunits in the central nervous system of the mollusc *Lymnaea*. *J Biol Chem* 281: 1680–1691, 2006.

Vorndran C, Minta A, Poenie M. New fluorescent calcium indicators designed for cytosolic retention or measuring calcium near membranes. *Biophys J* 69: 2112–2124, 1995.

Ward JM, Cockcroft VB, Lunt GG, Smillie FS, Wonnacott S. Methyllycaconitine–a selective probe for neuronal alpha-bungarotoxin binding-sites. *FEBS Lett* 270: 45–48, 1990.

Waterhouse AM, Procter JB, Martin DM, Clamp M, Barton GJ. Jalview version 2–a multiple sequence alignment editor and analysis workbench. *Bioinformatics* 25: 1189–1191, 2009.

Whim MD, Kaczmarek LK. Expression of a foreign G-protein coupled receptor modulates the excitability of the bag cell neurons of *Aplysia*. *Neurosci Lett* 258: 1–4, 1998.

White SH, Magoski NS. Acetylcholine-evoked afterdischarge in *Aplysia* bag cell neurons. *J Neurophysiol* 107: 2672–2685, 2012.

Xie Y, Cohen JB. Contributions of *Torpedo* nicotinic acetylcholine receptor γTrp-55 and δTrp-57 to agonist and competitive antagonist function. *J Biol Chem* 276: 2417–2426, 2001.

Yassin L, Gillo B, Kahan T, Halevi S, Eshel M, Treinin M. Characterization of the deg-3/des-2 receptor: a nicotinic acetylcholine receptor that mutates to cause neuronal degeneration. *Mol Cell Neurosci* 17: 589–599, 2001.

Zhong W, Gallivan JP, Zhang Y, Li L, Lester HA, Dougherty DA. From ab initio quantum mechanics to molecular neurobiology: a cation-pi binding site in the nicotinic receptor. *Proc Natl Acad Sci USA* 95: 12088–12093, 1998.